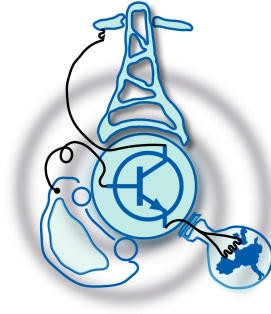


# Designing an extra-low power converter for an autonomous smoke detector.

by

Alejandro García Álvarez, [uo218991@uniovi.es](mailto:uo218991@uniovi.es)



Submitted to the Department of Electrical Engineering, Electronics,  
Computers and Systems

in partial fulfillment of the requirements for the degree of  
Master Course in Electrical Energy Conversion and Power Systems

at the

UNIVERSIDAD DE OVIEDO

June 2017

© Universidad de Oviedo 2017. All rights reserved.

Author .....  
Alejandro Garcia Alvarez

Certified by .....  
Antonio Javier Calleja Rodríguez  
Full Professor  
Thesis Supervisor

Certified by .....  
Daniel García Llera  
Tutor in NormaGrup Technology SA  
Thesis Supervisor



# Designing an extra-low power converter for an autonomous smoke detector.

by

Alejandro García Álvarez, [uo218991@uniovi.es](mailto:uo218991@uniovi.es)

Submitted to the Department of Electrical Engineering, Electronics, Computers and Systems

on July 5, 2017, in partial fulfillment of the requirements for the degree of

Master Course in Electrical Energy Conversion and Power Systems

## Abstract

In this thesis, an extra-low power supply which is used in a smoke detector is designed and implemented. This, involves a brief analysis among the possible topologies. After that, the design process is carried out fulfilling the requirements of the prototype which are related to the size, cost and validation of the power supply. Moreover, a simulation is made in order to see the performance of the converter easily and, then, the selection of the components regarding the final price of the prototype is shown. The schematic and the Printed Circuit Board (PCB) are described later pointing out the key concepts of the design. The different tests made to pass the regulations are explained and the results are shown to conclude if the work fulfils the established objectives. Finally, future works are mentioned taking into account the possible improvements and additional features of the prototype.

## Keywords

power supply, autonomous smoke detector, flyback converter, RC snubber, EMI, differential mode noise, common mode noise, TinySwitch, UNE EN 61000-3-2, UNE EN 14604, UNE EN 61558.

Thesis Supervisor: Antonio Javier Calleja Rodríguez

Title: Full Professor

Thesis Supervisor: Daniel García Llera

Title: Tutor in NormaGrup Technology SA

## Acknowledgments

Firstly, I would like to express my gratitude to my girlfriend, Covadonga, and my family, Luis, María Jesús and Isabel for the constant support during the Master and this final stage, the Master's Thesis.

I am grateful to Antonio Javier Calleja, my advisor, who helped me at any moment, and Manuel Rico Secades who got me in touch with NormaGrup Technology S.A. to arrange the intern-ship and Mikel Jaureguizar, the general manager, to accept me.

I would like to thank the workmates at the Research and Development department of NormaGrup Technology S.A., in particular, my co-advisor, Daniel García Llera, Fernando and the person who teached me many things about power electronics and helped me with the design process during my intern-ship, David Gacio. I am also grateful to the members of Quality department, specially Saray, who spent with me most of the time during my stay in the company and showed me the performance of the company.

Finally, I want to thank the teachers of the master all they have taught me.

# Contents

Table of symbols	12
Introduction	15
Objectives of the Master Thesis	17
State of the Art	19
<b>1 Study of possible topologies</b>	<b>21</b>
1.1 Switch mode power supplies (SMPS) . . . . .	21
1.1.1 Isolated Flyback converter . . . . .	21
1.1.2 Forward converter . . . . .	22
1.1.3 Half-bridge and full-bridge converters . . . . .	23
1.1.4 Resonant converters . . . . .	24
1.2 Linear power supplies . . . . .	25
1.3 Conclusion . . . . .	25
<b>2 Flyback converter: performance and characteristics</b>	<b>27</b>
2.1 The flyback converter . . . . .	27
2.2 TNY264GN: Characteristics and operation . . . . .	29
2.2.1 Functional description . . . . .	30
2.2.2 TinySwitch-II operation . . . . .	32
<b>3 Design of the converter</b>	<b>35</b>
3.1 Circuit and components calculation procedure . . . . .	35

3.1.1	Input capacitor and output diode selection . . . . .	35
3.1.2	TinySwitch and operation mode selection . . . . .	37
3.1.3	Primary inductance and transformer design . . . . .	39
3.1.4	RMS currents and output capacitor . . . . .	40
3.1.5	Feedback circuit and output postfilter . . . . .	41
3.2	Flyback Transformer . . . . .	41
3.2.1	Normative. UNE-EN 61558-1. Part 26. . . . .	41
3.2.2	Choice of the magnetic core . . . . .	43
3.2.3	Methodology and description of the process . . . . .	43
3.3	Complementary circuitry . . . . .	46
3.3.1	RC Snubber . . . . .	47
3.3.2	Primary RCD clamp . . . . .	49
3.3.3	Transient voltage suppressor (TVS) diode . . . . .	52
3.4	Electromagnetic Interferences (EMI) . . . . .	54
3.4.1	Types of EMI . . . . .	54
3.4.2	Measuring Conducted Emissions . . . . .	55
3.4.3	Types of noise . . . . .	57
3.4.4	Study of our system . . . . .	61
<b>4</b>	<b>Simulation</b>	<b>63</b>
<b>5</b>	<b>Components selection</b>	<b>69</b>
5.1	Grid connection and rectifier . . . . .	69
5.1.1	Terminal block . . . . .	69
5.1.2	Grid fuse . . . . .	70
5.1.3	Rectifier bridge . . . . .	70
5.2	EMI input filter . . . . .	70
5.3	Input capacitor . . . . .	71
5.4	RC snubber and clamp circuit . . . . .	73
5.4.1	RC snubber . . . . .	73
5.4.2	Clamping circuit . . . . .	73

5.5	TinySwitch . . . . .	73
5.6	Flyback transformer and decoupling capacitor . . . . .	74
5.6.1	Flyback transformer . . . . .	74
5.6.2	Decoupling capacitor . . . . .	75
5.7	Output diode and capacitor . . . . .	75
5.7.1	Output diode . . . . .	75
5.7.2	Output capacitor . . . . .	75
5.8	Optocoupler and feedback circuit . . . . .	76
5.9	Output indication LED . . . . .	77
5.10	Price of the prototype . . . . .	77
<b>6</b>	<b>Schematic, PCB design and final prototype</b>	<b>79</b>
6.1	Schematic design . . . . .	79
6.2	PCB design . . . . .	80
6.3	Final prototype . . . . .	82
<b>7</b>	<b>Tests, validation and regulation</b>	<b>85</b>
7.1	Oscilloscope tests . . . . .	85
7.1.1	No-load state and transient to ALARM state . . . . .	88
7.2	Conducted EMI test . . . . .	89
7.3	Thermal study . . . . .	90
7.4	Current harmonics validation. IEC61000-3-2 . . . . .	92
	<b>Conclusions</b>	<b>95</b>
	<b>Future developments</b>	<b>97</b>
	<b>Quality report</b>	<b>99</b>
	<b>Internship at NormaGrup Technology S.A</b>	<b>101</b>



# List of Figures

0-1	Smoke detection systems from NormaDet[20]	15
1-1	Flyback converter[3].	22
1-2	Forward converter[3].	23
1-3	Half-bridge topologies[3]	23
1-4	Resonant converter[7].	24
1-5	Curves of performance for resonant converter[7].	25
1-6	Linear power supply scheme[3].	26
2-1	Derivation of the flyback from the buck-boost converter [22].	28
2-2	CCM and DCM waveforms[15]	29
2-3	Functional block diagram of the TNY264GN	30
2-4	Operation at maximum and minimum loads[12].	32
3-1	Typical standby application application[12]	37
3-2	Horizontal coil former for E16/8/5	44
3-3	Winding area and insulation margins	45
3-4	Model of the trafo[17]	46
3-5	Turn-off waveform with the clamping circuit	47
3-6	RC snubber circuit[16].	48
3-7	RCD clamp circuit[16].	50
3-8	Typical waveform of drain-to-source voltage at turn-off[16].	51
3-9	Transil performance curves[6]	52
3-10	Peak pulse power vs exponential pulse duration curve[6].	53

3-11	Line Impedance Stabilization Network (LISN)[5]. . . . .	56
3-12	Differential mode noise transmission path[2]. . . . .	57
3-13	Comparison between ideal and real capacitors[5]. . . . .	58
3-14	Types of basic input filters [11] . . . . .	59
3-15	Common mode noise transmission path[2]. . . . .	60
3-16	Typical common mode choke[5]. . . . .	60
4-1	Open-loop simulation scheme . . . . .	64
4-2	Input voltage/current and output voltage . . . . .	65
4-3	Switching variables . . . . .	65
4-4	Open-loop output variables . . . . .	66
4-5	Clamping circuit open-loop curves . . . . .	67
6-1	Schematic of the prototype 2 . . . . .	80
6-2	PCB 1 . . . . .	81
6-3	PCB 2 . . . . .	82
6-4	Pictures of PCB 1 . . . . .	83
6-5	Pictures of the board for PCB 2 . . . . .	83
6-6	Pictures of final PCB 2 . . . . .	84
7-1	Complementary circuits effects at the turn-off . . . . .	86
7-2	Input voltage ripples . . . . .	87
7-3	Detail of ON/OFF control . . . . .	87
7-4	Transient to ALARM state . . . . .	88
7-5	Steady state (ALARM state) . . . . .	89
7-6	Frequency spectrum conducted EMI for PCB 1 . . . . .	90
7-7	Frequency spectrum for PCB 2 . . . . .	91
7-8	Thermal images of the PCB 1 . . . . .	91
7-9	Thermal images of the PCB 2 . . . . .	92
7-10	Report IEC61000-3-2 class D validation for PCB 2 . . . . .	94

# List of Tables

1	Commercial autonomous smoke detectors[19][10][8][21][14]. . . . .	19
3.1	Ferrite cores possibilities . . . . .	39
3.2	CTI intervals . . . . .	42
3.3	Creepage distances, insulating distances and distance through the insulation. Distances in mm. . . . .	44
3.4	RC snubber values of PCB 1 and PCB 2 . . . . .	49
5.1	Price of the prototype 2 . . . . .	78
7.1	Comparison PCB1, PCB2 and PCB2 at no-load . . . . .	89
7.2	Regulations validated for PCB 2 . . . . .	93



# Table of symbols

$DC_{MAX}$  Maximum Duty Cycle.

$I_{LIMIT}$  Current limit.

$f_r$  resonant frequency.

$f_s$  switching frequency.

$t_c$  Conduction time of the rectifier diode.

$t_{LEB}$  Leading Edge Blanking.

$t_{rr}$  Reverse Recovery Time.

$v_{or}$  Reflected Output Voltage.

**BP** ByPass.

**CCM** Continuous Conduction Mode.

**CTI** Comparative Tracking Index.

**DCM** Discontinuous Conduction Mode.

**EMI** A disturbance that happens in any circuit, component or electronic system produced by an external or internal electromagnetic radiation source.

**EN/UV** Enable/Undervoltage.

**LISN** Line Impedance Stabilization Network.

**PCB** Printed Circuit Board.

**PIV** Peak Inverse Voltage.

**S** Source.

**SMD** Surface Mount Device.

**SMPS** Switch Mode Power Supply.

**SPE** Series Pass Element.

**TVS** Transient Voltage Suppression.

# Introduction

Nowadays, the smoke, fire and toxic gases detection products are increasing rapidly due to requirements established by the security regulations. Domestic as much as industrial buildings need a robust smoke detection system in order to prevent conflagrations. Two types of smoke detectors configurations are widely used, the autonomous detector and the detector controlled by a fire central. The autonomous is less used for industrial buildings but it is used for domestic and small business applications.

Regarding the energy supply of the fire detection system, a main power supply is needed when all the detectors are controlled by a central control panel. However, the energy conversion takes on much importance in the case of the autonomous detectors because each individual detector has its own integrated power supply that involves a significant cost.

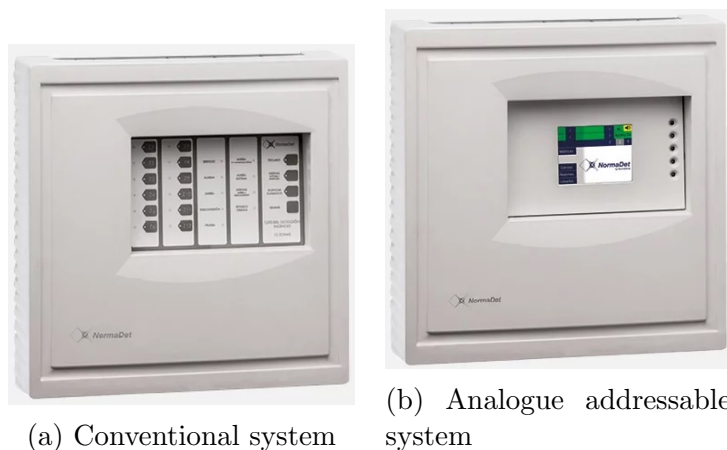


Figure 0-1: Smoke detection systems from NormaDet[20]

NormaGrup Technology S.A, an Asturian company which is the leader of emergency lightning in Spain and it also has a very high international relevance, has a

division, called NormaDet, specialised in fire detection and whose two main products are shown in figure 0-1. Both of them are centralised fire detection systems and have its own characteristics. The conventional system, defined by its toughness and quality, can control different lines or zones with several detectors, so, in case of alarm, it will not show exactly in which device but the line affected takes place the alarm. The addressable system has a higher capacity for control and supervision knowing exactly the state of each detector of the whole system.

However, the company has the aim of developing an autonomous smoke detector for domestic and small business applications. At first, its prototype was powered by a 9 V battery, but, due the regulations, a main power supply connected to the grid along with an alternative one are compulsory. Therefore, this project is intended to develop an isolated power supply which will be integrated inside the detector casing as the main power source keeping the battery as the auxiliary power supply.

# Objectives of the Master Thesis

The objectives of the Master Thesis can be classified as the technical objectives, proposed by the company because they are related to the product they want to develop, and the academic objectives, related with the knowledge and the final results I can achieve.

Starting from the technical objectives of the prototype, it should be pointed out that several requirements have to be fulfilled by the design:

## Size

The dimensions of the final prototype have to be equal than the 9 V battery because the smoke detector casing is already designed and the space destined for the battery has to be reused for the power supply. It is a critical requirement in terms of PCB design and the electric isolation.

## Price

As it is expected the company requires the cheapest design. Thus, this involves well known materials and components, an innovative design is not a preference. They prefer a tough and simple design in order to reduce the price of the product as much as possible.

## **Regulation**

The prototype has to pass the different standards and regulations related to power supplies. As this product can be commercialized in the future, the electrical security and the connection to the grid are the key points.

## **Efficiency**

Although the efficiency is always a significant characteristic of any power electronics design, it is not a priority in this case. The three requirements described above have more importance than the efficiency. First of all, the rated power of the power converter is 1 W, and in power electronics, the lower the rated power, the more difficult achieving a high efficiency of the design. For instance, if there is only 0.2 W of losses out of a rated power of 1 W, it involves a 80% of system efficiency.

## **Academic objectives**

Regarding the development of the thesis, my objectives are related to get more experience power electronics. Particularly, in terms of working in the laboratory with all the equipment, learning all the regulated tests and validations and knowing all the procedure of developing an electronic product which will be put on sale in the future. Moreover, the documentation of this kind of projects is a possibility of improving the English and writing skills. Finally, the opportunity of doing an intern-ship in one of the most important companies of the electronic manufacture sector is something which I am proud of it. Thus, trying to learn the maximum from the workmates and people from the research and development department during the stay is one of the main objectives.

# State of the Art

Regarding the autonomous smoke detection, there are several products in the market shown in the table 1, where the main specifications of the products are described.

Table 1: Commercial autonomous smoke detectors[19][10][8][21][14].

Manufacturer	Model	Power Supply	Voltage supply	No-load consumption	Alarm consumption	Regulation
COFEM	-	Alcaline battery	9 VDC	8 uA	15 mA	-
COFEM	-	Lithium battery	3 VDC	3 uA	-	EN - 14604
Schneider Electric	ARGUS	Ion-Lithium/Alcaline batt.	9 VDC	-	-	EN - 14604
Schneider Electric	ARGUS	Grid+Battery	230V/50 Hz + 9VDC	-	-	EN - 14604
VisioTech	SMK-500	Battery	9 VDC	-	-	-
Golmar	DOA - 21123005	Battery 6F22	9 VDC	10 uA	-	EN - 14604
EURA (MIRA)	BSC02936	Grid/Bat. 6LR61	230 V / 9 VDC	10 uA	20 mA	EN - 50194
EURA (MIRA)	BSC02937	Grid/Bat. 6LR61	230 V / 9 VDC	10 uA	30 mA	EN - 50194

Most of them are fed at 9 V and some of them as the ARGUS model from Schneider and two models from MIRA have also the possibility of grid connection. The consumption is similar in all of them, but the power consumption is higher for the MIRA detectors, which are also cheaper (around 10 €), than the COFEM detectors, between 15 and 20 €.

Then, in terms of power supplies, it is not very common finding them isolated from the whole system. For instance, RS Pro has a Embedded Switch Mode Power Supply (SMPS) [18] of 9 V and 1 W, the target features for the one developed in this project. Its input voltage range is 85-305 VAC. It meets the standards IEC61000, UL60950 and IEC60950 related to over output current protection, and short circuit protection and, regarding EMC, regulations UNE-EN 50561-1 and UNE-EN 55032 are fulfilled. So, the prototype designed in this project should pass, at least, the same standards.



# Chapter 1

## Study of possible topologies

In this section, several topologies are explained, pointing out the advantages and disadvantages for the particular application of this study. Finally, the most suitable topology is discussed taking into account the special characteristics of each case; the size, power and efficiency requirements and the cost of the whole system. Then, in the next chapter the chosen topology is explained in detail.

### 1.1 Switch mode power supplies (SMPS)

The use of switch mode topologies has reduced the size and has improved the efficiency of the power supplies. The transformers, inductors and capacitors have become smaller. It is possible due to an increase of the switching frequency operation although higher switching losses take place. Moreover, the resonant topologies, which ensure zero voltage or zero current at the transitions, are starting to be used, providing good power density for the same amount of power [3].

#### 1.1.1 Isolated Flyback converter

This topology, shown in figure 1-1 is commonly used in low power applications, up to 150 W, because of its simplicity and the reduced number of components. It uses a main magnetic component which is the couple inductor providing energy storage

and isolation. The energy is transferred to the secondary during the off-time of the switching element[3]. It is a low cost AC/DC converter which power is restricted by the high levels of energy at the output capacitor. For very low power, as it is the case of our application, the discontinuous mode of operation is usually used because of the lower current and voltage ripple at the output, the cheaper output rectifier diode and the reduced Electromagnetic Interference (EMI) and noise[4].

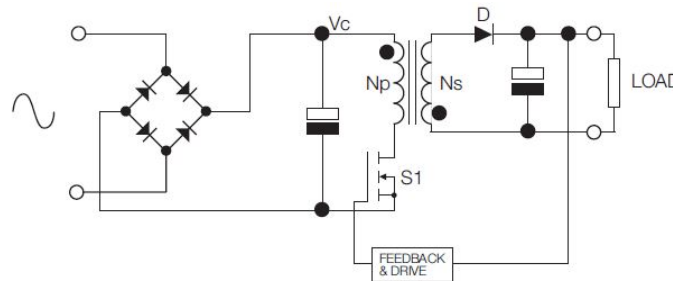


Figure 1-1: Flyback converter[3].

### 1.1.2 Forward converter

The typical power range of the forward converter is 100-300 W. This topology, unlike the flyback converter, has two magnetic components, a transformer and an output inductor. The energy is transferred to the secondary and the load at the on-time of the switching element. The forward converter is widely used in both AC power supplies and DC/DC topologies [3]. The transformer is different from the one used in flyback converters because it does not store the energy which, in this case, is stored in the output inductor and capacitor. The output inductor reduces the ripple current at the output capacitor and the transformer size is totally dependent on the the switching frequency and the power dissipation. A possible variation of this topology is the addition of another transistor to achieve higher current rating and to divide by two the voltage that the components have to withstand. The figure 1-2 shows the basic scheme of this topology.

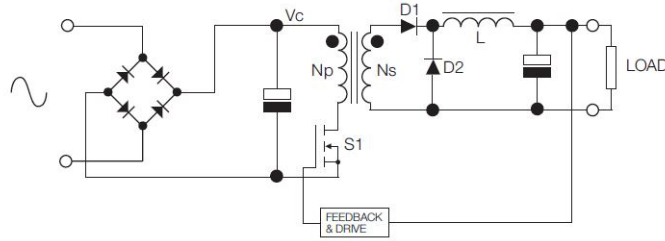
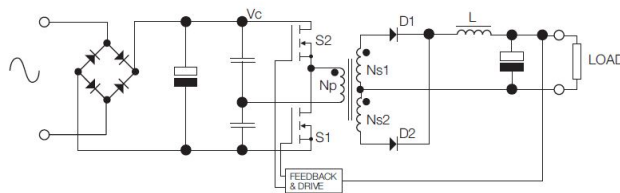


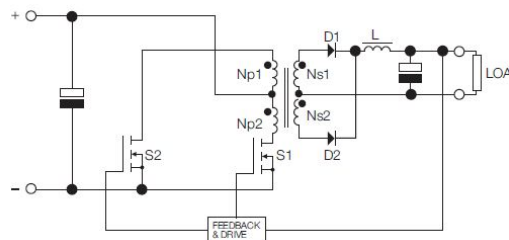
Figure 1-2: Forward converter[3].

### 1.1.3 Half-bridge and full-bridge converters

Half bridge converters have a power range between 150 and 1000 W. As in the case of the forward converter, this topology, shown in figure 1-3a, also uses a transformer and an output inductor, but the transformer is better used than in the forward case. The switching components work independently connecting the primary transformer both positive and negative with respect to the center point. The energy transfer take place during the on-time of each switching element due to a secondary winding which is divided in two parts. The advantage of this configuration is the double switching frequency seen by the secondary, which leads to a reduction in the volume of the output inductor and capacitor[3] . In higher power solutions a full bridge can be employed.



(a) Half bridge converter.



(b) Push-pull converter.

Figure 1-3: Half-bridge topologies[3]

Half and full-bridge topologies are widely used in AC input power supplies and also in low voltage bus converters. The push-pull configuration (figure 1-3b), usually used in DC/DC converters, has the same features as the half-bridge excepting the arrangement of the power switches that allows to halve the primary switching current.

### 1.1.4 Resonant converters

The resonant converters have a high efficiency, low EMI and high power density. The figure 1-4 shows a widely used topology for this type of converters. From a DC voltage input the switching bridge generates a square waveform that excites the resonant tank, which consists in a capacitor, an inductor and the magnetizing inductance of the transformer, then the rectifier gets again the DC output. The gain of the converter comes from the switching bridge gain (1 for Full-Bridge and 0.5 for Half-Bridge), the resonant tank gain and the transformer turns ratio ( $N_s/N_p$ ).

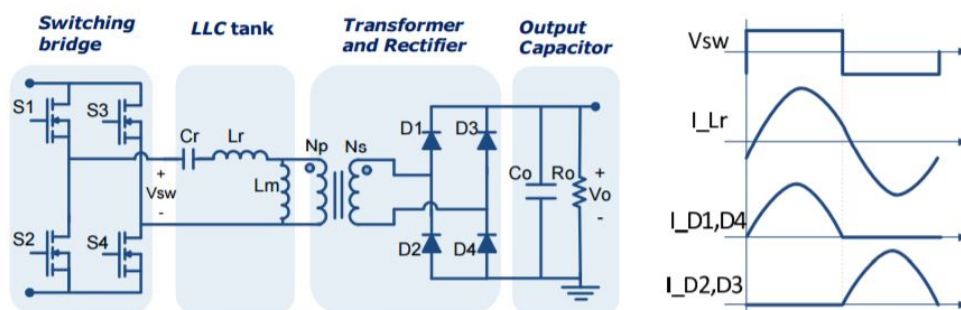


Figure 1-4: Resonant converter[7].

The resonant tank has a different gain with the normalized switching frequency ( $f_s$ ) for different values of quality factor  $Q$  and any value of modulation,  $m$ . The figure 1-5 shows the performance curves for a particular  $m$ . So, depending on the input voltage and the load the resonant converter has three operation modes since the resonant network gain is frequency modulated. The converter can operate at resonant frequency ( $f_r$ ),  $f_s=f_r$ , where the resonant tank has a unity gain and best optimized option and efficiency, so the transformer is designed to operate at this point at nominal input and output voltages [7]. Another mode of operation is working below resonant frequency,  $f_s < f_r$ , when a step up or boost converter is required due to lower input

voltage. And finally, if the converter works above resonant frequency,  $f_s > f_r$ , means that the input voltage is higher, so a step down gain or buck performance is needed. Since, the last operation mode is the suitable for our particular case, it will be taken into account at the choice of the power converter topology .

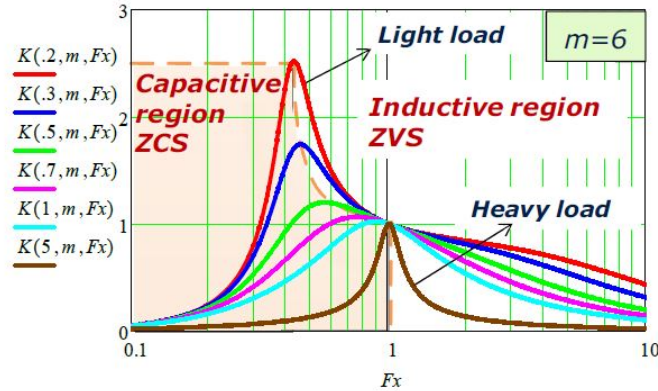


Figure 1-5: Curves of performance for resonant converter[7].

## 1.2 Linear power supplies

Linear power supplies (figure 1-6) are only used in specific applications for low noise requirements (audio-visual, medical, communication and measurement devices), or in very low power applications where a simple input transformer rectifier is enough and provides low cost (alarm panels). The transformer reduces the voltage at levels that can be used, the secondary voltage is rectified and a Series Pass Element (SPE) is employed to regulate the system. The advantages of this topology, as it is said above, are low noise, reliability and low cost but some drawbacks are the size, the weight and the inefficiency when the difference between the input and output voltage is large. Moreover, a linear regulator generates a great amount of heat.

## 1.3 Conclusion

Among the different topologies the more suitable one is the isolated flyback converter. It is the cheapest one out of the SMPS because it is the one that has less components

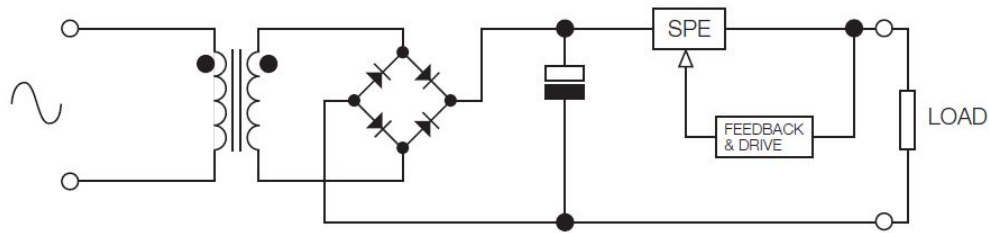


Figure 1-6: Linear power supply scheme[3].

and the lowest power rating (up to 150 W). Moreover, compared to the linear, it is better in terms of size which is an important requirement, and, although the efficiency is not a priority, the losses are lower in the flyback converter.

# Chapter 2

## Flyback converter: performance and characteristics

In this section, a brief review about the basic concepts of the flyback converter is made. The main characteristics, in particular, its performance and the typical waveforms are described. The modes of operation are also explained and discussed taking into account the advantages and disadvantages of each of them regarding our specific case. Finally, a description of the TinySwitch, pointing out its most significant features, and its operation being part of the whole system is presented.

### 2.1 The flyback converter

As it is known, the flyback converter is an isolated version of the buck-boost converter and its derivation is shown in figure 2-1. From the buck-boost converter, the first change is the construction of the inductor by using two wires with a unity turns ratio but the basic function of the resultant transformer is the same as the original inductor. Then the connection between windings is removed, the primary winding will be used when the switching element conducts and the secondary winding will conduct when the diode is also conducting. The total current of the obtained circuit is equal to the original one but the distribution between the windings is different now. Although the symbol used is the ideal transformer symbol, it represents in this case a “two winding

inductor”, also called “flyback transformer”. Unlike the ideal transformer, the current does not flow at the same time through both windings, the polarity terminals of the transformer are reversed, as it can be seen in figure, to obtain a positive voltage and a 1:n turns ratio is chosen.

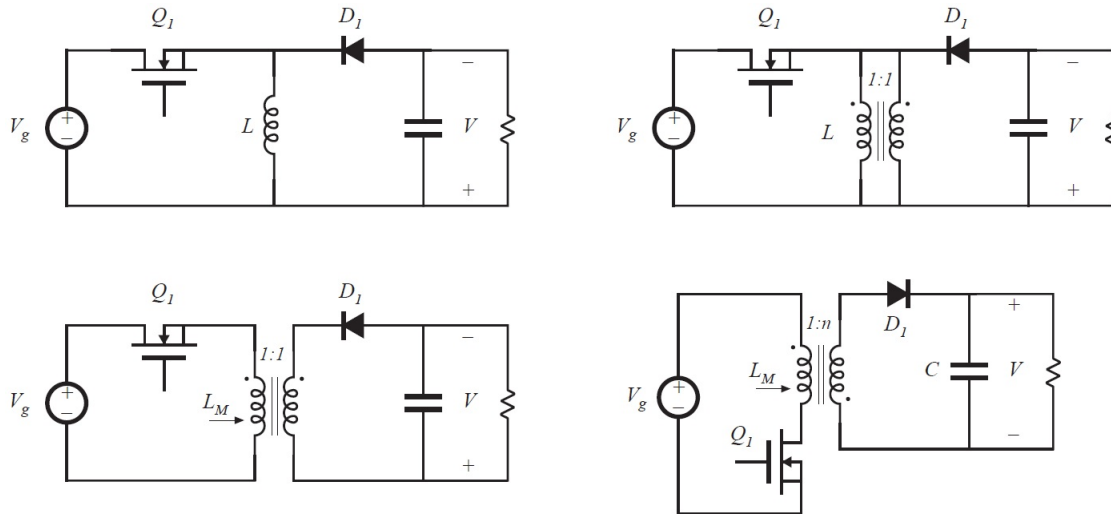


Figure 2-1: Derivation of the flyback from the buck-boost converter [22].

There are two basic energy-transfer modes of operation [15]. In the first one, called Continuous Conduction Mode (CCM), part of the energy stored in the flyback remains in the transformer when the next ON period starts. In the second, called Discontinuous Conduction Mode (DCM), all the energy is transferred to the load during the OFF period. There is another Critical Conduction Mode (CRM) or Transition Mode (TM), which is at the boundary between the other two modes, where the energy stored just reaches zero at the end of the period.

In figure 2-2 the waveforms in CCM and DCM are shown. In DCM the current through the MOSFET starts at zero and reaches a peak that is around twice peak current in the CCM case. At the turn-off the secondary current reaches zero and remains at zero until the next period. Thus, a flyback which is operating at DCM needs a smaller inductance than the CCM because of this higher current ripple.

In terms of the losses in the MOSFET, the DCM has a worst performance due to the higher RMS current that also produce high losses in the primary and secondary capacitors and in the primary clamp. Thus, DCM requires a larger EMI filter and

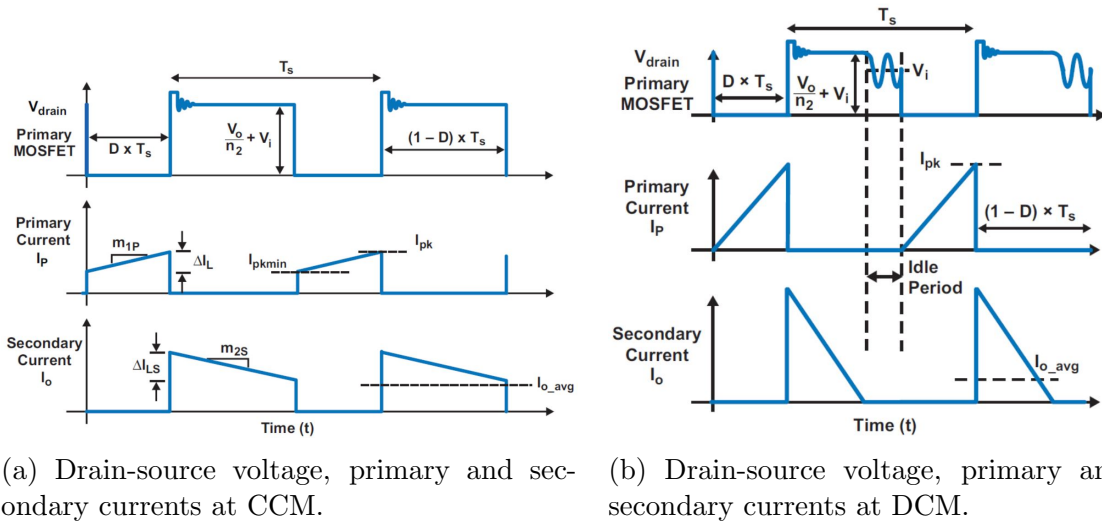


Figure 2-2: CCM and DCM waveforms[15]

output filter. However, it has not diode reverse recovery losses and there are some advantages related to control issues. The flyback topology is delivered to the load only during the OFF time of the control switch, so any control action during the on time is delayed to the next cycle. If there is CCM, facing an increase in load the output voltage is reduced, so the controller increases the ON time to store more energy. Increasing the ON time, the OFF time is reduced, which implies a reduction in the energy delivered to the load the first few cycles with the resultant large output voltage drop. The regulation returns when the energy from longer ON time is transferred to the load over several cycles [15]. In small signal analysis, this effect is called right-half-plane zero (RHPZ) and it does not take place in DCM, which is an advantage.

## 2.2 TNY264GN: Characteristics and operation

In this chapter, the main characteristics and the operation mode of the TinySwitch from Power Integrations are explained. This integrated circuit is defined as a low power off-line switcher and it stands out among the rest of similar chips because of its low cost and better performance. Generally, it has a fully integrated auto-restart for short circuit and open loop fault protection, a programmable line under voltage detection that prevents power on/off glitches, high frequency operation (132 kHz)

that allows the reduction of the transformer size.

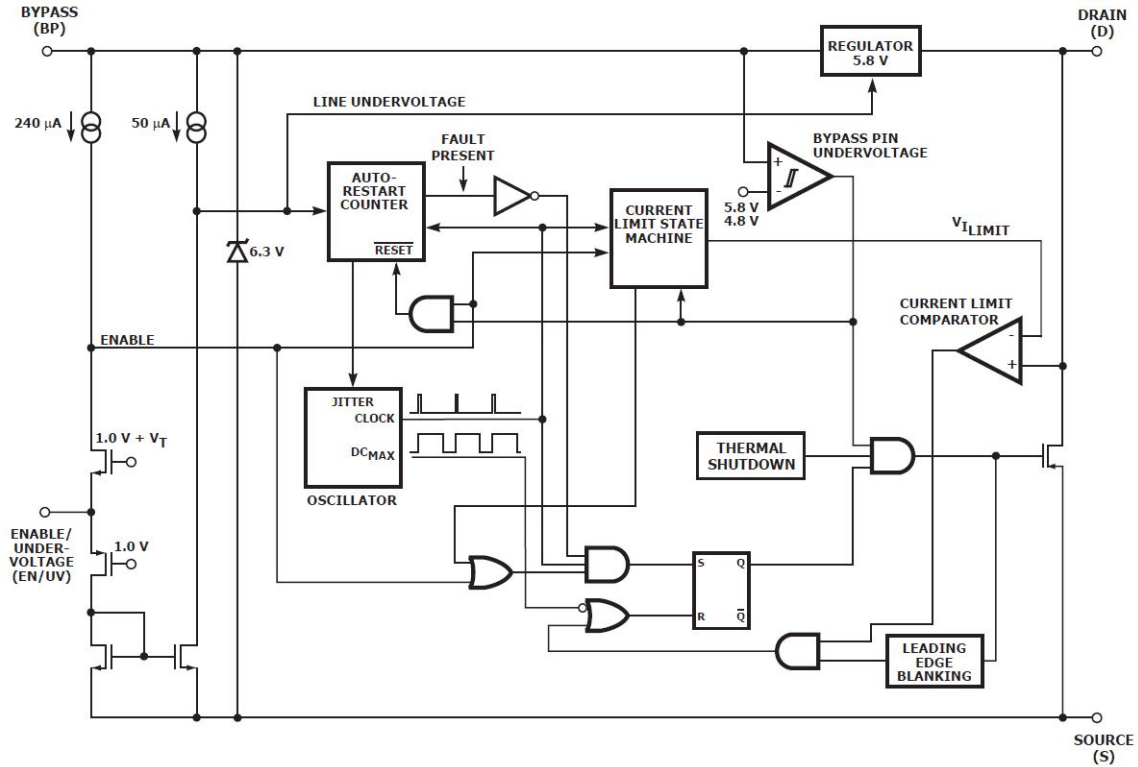


Figure 2-3: Functional block diagram of the TNY264GN

## 2.2.1 Functional description

Unlike the conventional PWM controllers, TinySwitch-II uses a simple ON/OFF control to regulate the output voltage.

Looking at the functional block diagram of the TNY264GN in figure 2-3, some of its functionalities are described.

### Oscillator, enable circuit and current limited state machine

From the oscillator two signals are generated, the Maximum Duty Cycle ( $DC_{MAX}$ ) and the clock signal that indicates the beginning of every cycle. A special feature of this controller is the addition of a small amount of frequency jitter at 8 kHz which minimizes the EMI. The function of the bypass capacitor (typically 100 nF) placed between the Bypass (BP) pin, is to be charged to 5.8 V absorbing current from the

drain pin when the MOSFET is off, and it represents the internal supply voltage for the integrated circuit [12]. Two current sources go out from BP. One of them provide a current of  $240 \mu A$  that pass through a source follower which purpose is to set a voltage of 1 V at the Enable/Undervoltage (EN/UV) pin, whatever is the voltage between BP and Source (S). When the current out of this pin is greater than  $240 \mu A$ , a low logic level is generated, so the output of the enable circuit is disabled and the MOSFET is turned off for that cycle. Since this state is only sampled at the beginning, any change during the remainder of the cycle is ignored.

The current limit state machine reduces the current limit value by discrete amounts at light loads. Under most operating conditions, the low impedance of the source follower keeps the EN/UV pin voltage to 1 V. This improves the time response of the optocoupler connected to this pin.

### **Internal voltage regulator and ByPass pin**

As it is said above the bypass capacitor is charged by the 5.8 V regulator that draws current from the drain pin when the MOSFET is off. The low energy consumption of the internal circuitry allow this type of supply, a  $0.1 \mu F$  capacitor is enough. Moreover, there is a shunt regulator clamping the bypass capacitor at 6.3 V when the current provided to the BP pin comes from an external resistor. The under-voltage circuitry disables the power MOSFET when the BP pin voltage drops below 4.8 V and following a hysteresis control, it does not work until the voltage rise to 5.8 V [12]. There is also a threshold based on hysteresis for the temperature protection, which has a value of  $135 \text{ }^\circ\text{C}$  to disable the MOSFET and  $70 \text{ }^\circ\text{C}$  to enable it again. The current limit circuit disables the MOSFET for the rest of the cycle if it senses a higher current than the internal threshold of Current limit ( $I_{LIMIT}$ ). A interesting feature is the Leading Edge Blanking ( $t_{LEB}$ ) circuit which inhibits the current limit comparator for a short time after the MOSFET turns on, to avoid a possible turn off due to current spikes.

## Auto-restart function and line under-voltage sense circuit

When a fault takes place such as an overload, an output short circuit or an open loop condition, the TinySwitch enters in auto-restart mode. It means, an internal counter clocked by the oscillator gets reset when the EN/UV pin is pulled low, but it is not pulled low during 50 ms, the MOSFET is disabled for 850 ms and then it tries to remove the fault again. In case of under-voltage condition, the MOSFET is disabled until the condition is removed.

### 2.2.2 TinySwitch-II operation

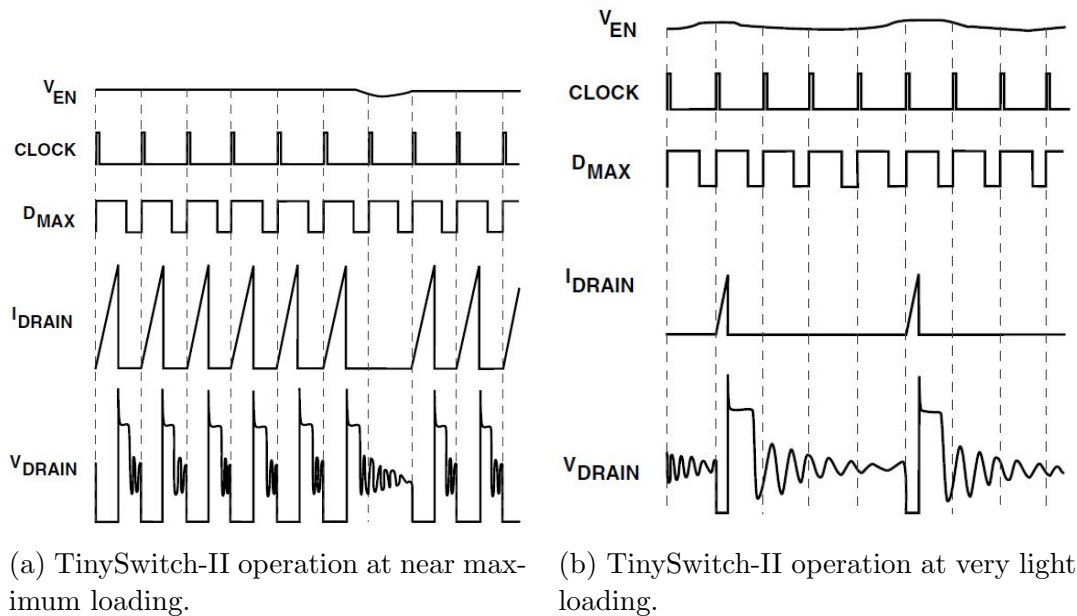


Figure 2-4: Operation at maximum and minimum loads[12].

As it has been explained this devices operate in current limit mode. The oscillator turns the MOSFET on at the beginning of each cycle and it is turned-off when the current through the MOSFET reaches the  $I_{LIMIT}$  or the  $DC_{MAX}$  is reached. Since the highest current limit and the frequency of the TinySwitch-II is constant, the power delivered is proportional to the primary of the transformer inductance and the current squared. The enable signal is generated in the secondary by comparing the output voltage of the power supply with a reference voltage. Particularly, EN/UV pin is high

if the voltage of the power supply is less than the reference voltage set by the zener diode [12]. When the output voltage exceeds the reference voltage the optocoupler LED which is in series with the zener, starts to conduct, pulling the EN/UV pin low.

Figures 2-4a and 2-4b shows the comparison between a situation near to maximum load and a very light load situation, respectively.

When there is a voltage lower than the limit for the EN/UV pin, less current go through mirror current and go below  $50 \mu A$  the line under-voltage signal is activated.



# Chapter 3

## Design of the converter

In this section, the complete design of the converter is carried out. The process is explained in detail, starting from the calculation of the converter parameters and the design of the transformer[4]. Then, the complementary but necessary circuitry is described choosing the best topology. Finally, a brief description of the EMI and the solutions adopted to remove it partially.

### 3.1 Circuit and components calculation procedure

The requirements of the system are the first step in the methodology design of a power supply. In this case an Universal input voltage is needed, so, it means, an range input voltage from  $85 V_{RMS}$  to  $265 V_{RMS}$ . Although the system will be able to work at any standard input frequency, the chosen one is  $50 \text{ Hz}$ <sup>1</sup>. As it is already known the output voltage is  $9 \text{ V}$  and the maximum output power should be less than  $1 \text{ W}$ . There is no efficiency requirement at first.

#### 3.1.1 Input capacitor and output diode selection

Schottky diodes (used up to  $7.5 \text{ V}$ ) and UltraFast diodes (beyond  $7.5 \text{ V}$ ) have the best efficiency in general terms [4]. However, the efficiency is not a objective of this

---

<sup>1</sup>Some tests were made at  $60 \text{ Hz}$

work. The cost is one of the main concerns. Thus, a fast diode is chosen ,which is suitable for a DCM of operation as it will be explained later. The selected diode would have a forward voltage drop,  $V_D$ , between 1 V and 1.7 V. So, the percentage of power losses through the output diode over the output voltage can be calculated at the worst case in equation 3.1.

$$\eta = \frac{V_D}{V_o} \cdot 100 = \frac{1.7 V}{9 V} \cdot 100 = 18.9 \% \quad (3.1)$$

A solution for the voltage peaks at the MOSFET's turn off is needed. It can be based in a RCD clamp circuit or a Transient Voltage Suppression (TVS) diode. Choosing a RCD clamp circuit, you have more freedom and flexibility over the design, in terms of power dissipation and maximum voltage peak allowed. However, the TVS will only dissipate energy when it clamps the voltage,it means when it is in reverse conduction, so the losses appear when it is acting. An RC snubber is also taken into account to counteract the ringing due to the resonance of parasitic elements of the circuit at the turn off. The EMI will be attenuated with these complementary circuits that will be explained later. The figure 3-1 shows the expected turn-off waveform.

It is supposed that the energy losses due to these circuits along with the output diode are around 35 %. So, the power supply would have an efficiency of 65 %. Afterwards, by carrying out different tests and measurements, a final decision about this circuits is made and the real efficiency of the power supply is obtained.

The maximum DC voltage, after the diode rectifier, is calculated in equation 3.2

$$V_{max} = \sqrt{2} \cdot V_{AC_{max}} = 374.77 V \quad (3.2)$$

where  $V_{AC_{max}}=265 V$ .

For Universal input voltage, the selected input storage capacitor depends on the required maximum voltage ripple at the input, a range between  $2 \mu F$  and  $4.7 \mu F$  can be suitable[4]. A  $4.7 \mu F$ , 400 V capacitor is chosen to get the lower ripple. Then, in the Components Selection chapter the choice of a specific capacitor is justified.

The Conduction Time ( $t_c$ ) of the rectifier is supposed to 2 ms. Then, the simu-

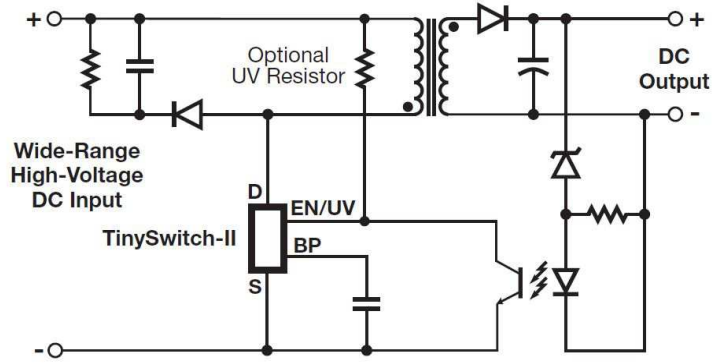


Figure 3-1: Typical standby application application[12]

lation results will give us the values. Thus, the minimum DC voltage is calculated taking into account the estimated efficiency of the system 65 %.

$$V_{min} = \sqrt{(2 \cdot V_{AC_{min}}^2) - \frac{2 \cdot P_o \cdot \left(\frac{1}{2f_{grid}} - t_c\right)}{C_{IN} \cdot \eta_{PS}}} = 95.94 V \quad (3.3)$$

where  $V_{AC_{min}}$  is 85  $V_{RMS}$ ,  $P_o$  is 1 W,  $f_{grid}$  is 50 Hz.

The output diode Peak Inverse Voltage (PIV) is needed for calculating the Reflected Output Voltage ( $v_{or}$ ) in the equation 3.4. It is supposed a peak repetitive reverse voltage of 200 V, so the PIV is the 80 % of this value.

$$V_{or} = V_{max} \cdot \frac{V_o + V_{D_{outdiode}}}{PIV - V_o} = 26.56 V \quad (3.4)$$

To keep  $V_{DRAIN}$  below 650 V (recommended level), the reflected output voltage should be kept below 150 V.

### 3.1.2 TinySwitch and operation mode selection

At this point, the TinySwitch-II family is chosen. Among the different models, the TNY264GN is chosen for the first prototype because it is available in the laboratory although the TNY263, which has a lower rated power, would more suitable for the power requirements of the system. The design of the whole converter is based in the primary peak current ( $I_p$ ), the  $DC_{MAX}$  because these parameters are key points

of the internal performance of the TinySwitch as it has been explained before. The minimum of the current limit specified by the datasheet,  $I_{limit_{MIN}}$ , multiplied by its over temperature derating factor of 90 % results in  $I_p$ , as the equation 3.5 shows.

$$I_p = 0.9 \cdot I_{limit_{MIN}} = 0.9 \cdot 233 \text{ mA} = 0.2097 \text{ A} \quad (3.5)$$

The maximum duty cycle is calculated in the equation 3.6 .

$$D_{max} = \frac{2 \cdot P_o}{\eta_{PS} \cdot V_{min} \cdot I_p} = 0.153 \quad (3.6)$$

From [4], a variable called  $K_{DP}$  is calculated, it represents the ratio between the off-time of the switch and the reset time of the core. If  $K_{DP} \geq 1$ , the system is going to operate in DCM under most of situations but there is a possibility of CCM. If  $K_{DP} < 1$ , the system provides higher output power. In this mode, a Schottky output diode should be used to prevent long reverse recovery times that could exceed leading edge blanking period ( $t_{LEB}$ ). In equation 3.7, this factor is calculated.

$$K_{DP} = \frac{V_{or} \cdot (1 - D_{max})}{V_{min} - D_{max}} = 1.53 \quad (3.7)$$

The DCM is widely used in several applications for low video noise and very low output ripple, especially in low power applications. To check for fully discontinuous operation the  $K_{DP}$  has to be greater than the value of the equation 3.8.

$$K_{DP} \leq \frac{1 - D_{max}}{0.67 - D_{max}} = 1.639 \quad (3.8)$$

As it can be seen, the fully discontinuous operation cannot be guaranteed at any situation, so the output reflected voltage is recalculated in equation 3.9 where  $K_{DP}$  is set to 1.639

$$V_{or} = \frac{K_{DP} \cdot V_{min} \cdot D_{max}}{1 - D_{max}} = 28.44 \text{ V} \quad (3.9)$$

$V_{or}$  should be kept below 150 V because the maximum recommended voltage between MOSFET's drain and source is 650 V.

Once the fully DCM is achieved, the primary inductance is calculated.

### 3.1.3 Primary inductance and transformer design

The commutation frequency is set to 124 kHz, the minimum output frequency of the integrated circuit, though the typical frequency is 132 kHz.

Most of the system losses take place in the secondary side due to the output diode and the clamp/snubber circuits losses, so there is a loss allocation factor,  $Z$ , which value is 0 if all losses are in primary side and 1 if they are in the secondary side. The primary inductance is calculate in equation 3.10.

$$L_p = \frac{P_o}{I_p^2 \cdot f s_{min} \cdot \frac{1}{2 \cdot 0.9}} \cdot \frac{Z \cdot (1 - \eta) + \eta}{\eta} = 5.087 \cdot 10^{-4} H = 508.7 \mu H \quad (3.10)$$

The turns ratio,  $N_p/N_s$  is calculated in equation 3.11.

$$\frac{N_p}{N_s} = \frac{V_{or}}{V_o + V_D} = 2.658 \quad (3.11)$$

For this first calculation and the first prototype the ungapped core E16/8/5 is chosen, although, in coming prototypes other cores are evaluated. The table 3.1 shows different data cores.

Table 3.1: Ferrite cores possibilities

Core size	$A_e$ (mm <sup>2</sup> )	$A_{e_{min}}$ (mm <sup>2</sup> )	$A_L$ N87 material(nH)	$l_e$ (mm)
E 16/8/5 (EF16)	20.1	19.4	1000	37.6
E 14/8/4	15.5	13.1	860 (N27)	33.9
E 13/7/4 (EF 12.6)	12.4	12.2	850	29.6
E 10/5.5/5	10.9	10.4	800	26.3

The primary turns are calculated in equation 3.12. The peak flux density must not exceed the 3000 gauss (300 mT), but, in this case, it is limited to 2500 gauss for avoiding magnetic saturation and low audio noise designs[4].  $I'_p$  is equal to the maximum value of  $I_{LIMIT}$ , 0.267 A. The secondary turns are calculated in 3.13.

$$N_p = I'_p \cdot \frac{L_p}{B_p \cdot A_{e_{min}}} = 28.006 = 28 \text{ turns} \quad (3.12)$$

$$N_s = \frac{N_p}{\frac{N_p}{N_s}} = 10.54 = 11 \text{ turns} \quad (3.13)$$

### 3.1.4 RMS currents and output capacitor

The primary and secondary RMS currents,  $I_{RMS}$  and  $I_{SRMS}$ , are calculated in equations 3.14 and 3.15 respectively.

$$I_{RMS} = \sqrt{D_{max} \cdot \frac{I_p'^2}{3}} = 0.06 \text{ A} \quad (3.14)$$

$$I_{SRMS} = I_{SP} \cdot \sqrt{\frac{1 - D_{max}}{3 \cdot K_{DP}}} = 0.295 \text{ A} \quad (3.15)$$

where

$$I_{SP} = I'_p \cdot \frac{N_p}{N_s} = 0.71 \text{ A} \quad (3.16)$$

Looking at this values the wire gauge for primary and secondary windings is chosen. It is recommendable not to use a wire thinner than 36 AWG (0.127 mm diameter) to prevent excessive winding capacitance and improve manufacturability.

The output short circuit current  $I_{OS}$  (equation 3.17) is calculated by applying a conversion factor (k) to the RMS current,  $I_{SP}$ . This factor is obtained by empirical measurements: k=0.9 for Schottky diode and k=0.8 for fast diode.

$$IOS = I_{SP} \cdot k = 0.568 \text{ A} \quad (3.17)$$

Then the DC current rating for the diode  $I_D$  has to be checked and , if necessary, other diode should be chosen.

The output capacitor depends on the output ripple current,  $I_{RIPPLE}$  (equation 3.18)

$$I_{RIPPLE} = \sqrt{I_{SRMS}^2 - I_O^2} = 0.273 \text{ A} \quad (3.18)$$

The output capacitor must have a RMS current rating equal to or larger than this value of current ripple. A low ESR electrolytic capacitor is recommendable.

### 3.1.5 Feedback circuit and output postfilter

The output voltage should be sensed between the electrolytic capacitor and the possible output postfilter in order to reduce somewhat the current ripple to meet requirements. After some tests the use of a LC output filter is evaluated. The feedback loop needs a Zener diode in series with the optocoupler LED, so the reverse voltage zener is calculated in equation 3.19

$$V_Z = V_o - V_{LED} = 8 \text{ V} \quad (3.19)$$

where  $V_{LED}$  is around 1 V. Then, specific components will be chosen and the exact values of these calculations are obtained.

## 3.2 Flyback Transformer

Since the value of the primary inductance (508.7  $\mu\text{H}$ ) and the turns ratio (2.65) are known, the procedure of making the flyback transformer is explained in detail in this section. The different options in terms of size of the magnetic core and possible orientations of the coil former (vertical and horizontal), the regulations over isolation inside the transformers and the most common winding techniques to obtain a good performance transformer are analysed.

### 3.2.1 Normative. UNE-EN 61558-1. Part 26.

This regulation is equivalent to IEC 61558-1:2005. “Safety of power transformers, power supplies, reactors and similar products. Part 1: General requirements and

tests”, where some concepts and parameters related to the power transformers are defined. In printed circuits where can exist danger the distance between active parts of the circuit follows the same regulation. All the numerical values are shown in the tables 13, C.1 and D.1 of this regulation.

The following definitions are needed to understand the tables:

- **Creepage distance:** It is the shortest distance (through the air) along the surface of an insulating material between two conductive parts.
- **Clearance:** It is the shortest distance through the air between two conductive parts.

These two parameters depend on the operating voltage and the clearance also depends on the type of the insulating material which is classified in the following table 3.2

Table 3.2: CTI intervals

<b>Group I</b>	<b>Group II</b>	<b>Group IIIa</b>	<b>Group IIIb</b>
CTI >600	600 >CTI >400	400 >CTI >175	175 >CTI >100

The higher the Comparative Tracking Index (CTI) value, the smaller the creepage distance can be, so, a better insulating material is. Depending on the electrical insulation tape used for separate the primary and secondary windings, the security distances are chosen.

Another important concept is the pollution degree. It establishes the pollution level that can appear inside the device. There can be a high pollution on the place the transformer is, so the insulation parameters will be more restricted. The pollution in this context is defined as:

- **Pollution:** Any addition of solid, liquid or gaseous strange substance that involves a reduction in the dielectric properties or in the superficial resistivity of the insulation.

Four pollution degrees are established:

- Degree 1: Any pollution or only no conductive dry pollution.
- Degree 2: Only no conductive pollution is produced and, occasionally, it can be conductive due to the condensation.
- Degree 3: Conductive pollution or no conductive pollution that can be conductive due to condensation
- Degree 4: The pollution produces a persistent conductivity produced by the conductive dust, the rain or the snow.

### 3.2.2 Choice of the magnetic core

The high operation frequency of the TNY264GN allows to use small topologies for the flyback transformers like E13 or E16 cores. The reduced space requirement of the system would involve the utilization of the smallest core, but there is other significant issue that have to be taken into account, the insulation. By using E16/8/5, there is a greater area for fulfilling the insulation regulations than the E13/7/4 case, so it is the first option.

The coil former can be horizontal or vertical. The horizontal one has more space between primary and secondary terminals than the vertical one, so it is used in the first prototype (PCB 1) of the converter for analysing and studying its performance. Figure 3-2 shows the dimensions of the horizontal coil former for the E16/8/5.

Even so, in the second prototype (PCB 2) a vertical coil former for the E16/8/5 is used to reduce space at the PCB. Choosing a new material for the magnetic core has no sense in this work because the objective is a well-known and cheapest prototype. So, the typical N27 based in MnZn is chosen.

### 3.2.3 Methodology and description of the process

In our case, the insulation tape is classified in the group I level (CTI 600) and it is supposed a pollution level 2. Thus, the table 3.3, extracted from the normative,

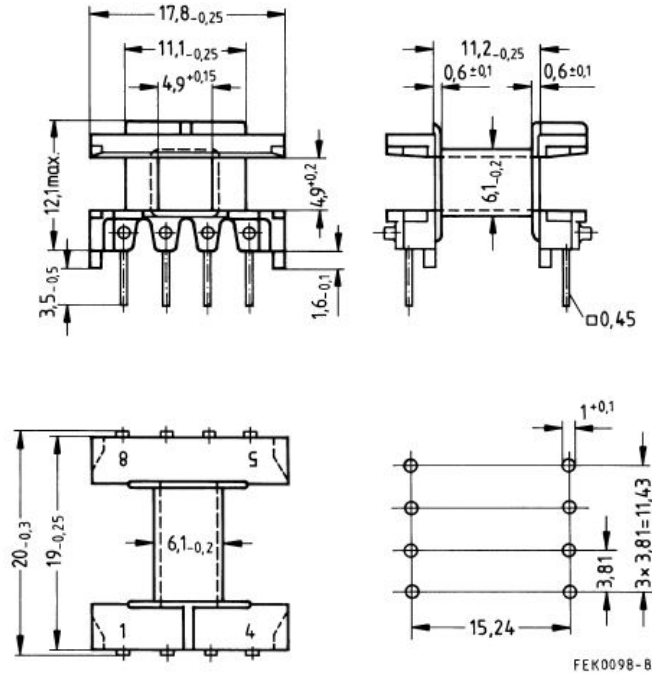


Figure 3-2: Horizontal coil former for E16/8/5

shows the suitable values for this conditions. The distance trough the insulation is made by 3 thin layers glued between primary and secondary windings, so the number used is the one inside the square bracket and it must be reduced a third of its value when the transformer has a nominal power lower than 25 VA. The operating voltage is the maximum DC voltage (380 V), so the values of the table between 300 V and 600 V are interpolated to obtain the suitable distances for this particular system.

Table 3.3: Creepage distances, insulating distances and distance through the insulation. Distances in mm.

	300 V		600 V		380 V	
	d	ldf	d	ldf	d	ldf
Creepage distance and insulating distance between active parts of primary windings and active parts of secondary windings.	Through the windings varnish					
	3,0	3,0	5,5	6,0	3,7	3,8
	Not through the varnish (between pins)					
	5,5	5,5	8,0	8,0	6,2	6,2
Distance through the insulation between primary circuits and secondary circuits	[0,16]		[0,19]		[0,17]	

Looking at the figure 3-2 the distance between pins is around 15 mm there is no restriction regarding the insulating distance and the creepage distance. The creepage

distance between windings is fulfilled by making thinner the winding area (B) of the coil former. It is appreciated in figure 3-4 how the margin (A) is the half of the creepage distance ( $ldf$ ). Thus, the procedure is the following:

1. A thin band of sticker paper is rolled on both margins to mark out the primary winding area.
2. The primary winding is wound up.
3. The insulating tape, which has the same width of the coil former shaft, is rolled over 3 turns.
4. The thin bands of paper are rolled to delimit the secondary winding area.
5. The secondary is wound up.
6. The core is inserted in the coil former, a very thin insulating tape band is rolled around the core and everything is fixed with glue.

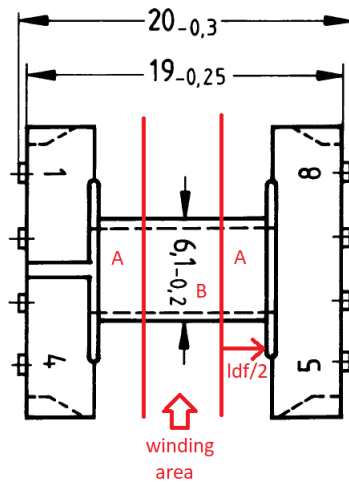


Figure 3-3: Winding area and insulation margins

### Measurements and characterization

Once the flyback transformer prototype is made some measurements are carried out in order to check the values of it by using the LCR meter. First of all, the primary

inductance is measured by connecting the LCR meter, at 100 kHz, to the primary side terminals, the value obtained is  $534 \mu\text{H}$  ( $460 \mu\text{H}$  for the vertical transformer). Then, the same procedure for the secondary inductance, obtaining a value of  $75.8 \mu\text{H}$  ( $41.5 \mu\text{H}$  for vertical transformer). This value is lower than the theoretical one calculated above, but it is decided to go on with it. Finally, the leakage inductance, which is measured by short-circuiting the secondary side and connecting the LCR gauges to the primary side of the transformer. A  $65.8 \mu\text{H}$  ( $44.5 \mu\text{H}$  for vertical transformer) is obtained which involves a 12 % (9.67 %) of the primary inductance. A 10 % of dispersion inductance is a typical value. The following calculations are made using the values for the horizontal coil former case, the same for the vertical coil former.

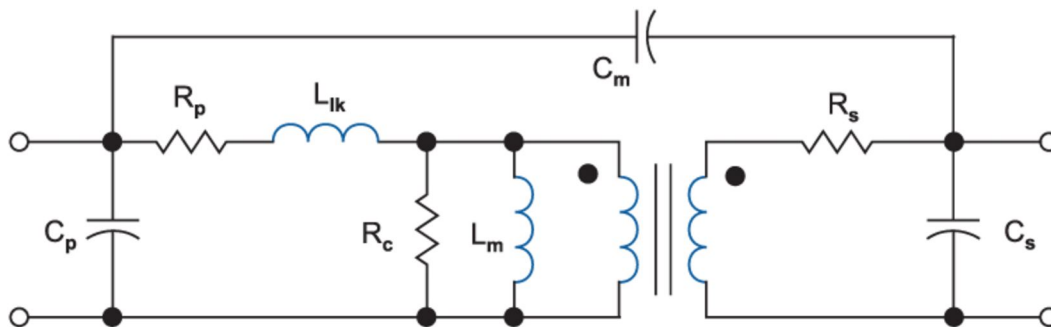


Figure 3-4: Model of the trafo[17]

### 3.3 Complementary circuitry

In this section, the design of this complementary circuitry is carried out by analysing the first tests waveforms at the oscilloscope. All the options are tested in the circuit and finally, a decision is made depending on the pros and cons of each one. The function of this circuitry is to allow the main circuit to work at the whole voltage range and to reduce the EMI emitted during its performance.

### 3.3.1 RC Snubber

The necessity of this circuit comes from the oscillations that take place at the turn-off of the switch. The figure 3-5 shows this ringing produced by the parasitic elements of the components, mainly due to the leakage inductance of the flyback transformer. In this case, there is only the clamping circuit implemented. Afterwards, a comparison between the effects of each sub-circuit are explained.

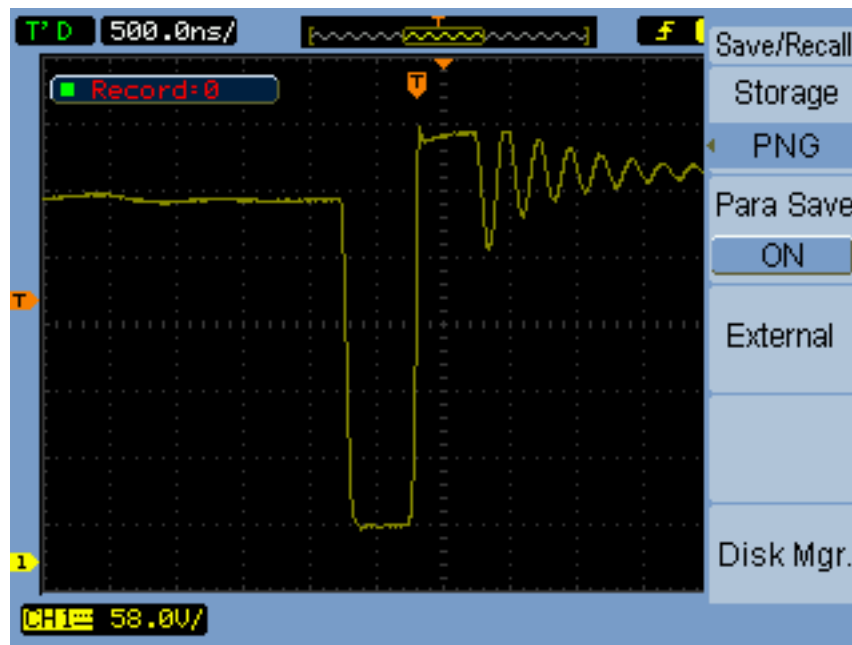


Figure 3-5: Turn-off waveform with the clamping circuit

Although many people usually assume the value of the leakage inductance as the 1% of the magnetizing inductance, it is sometimes greater than an order of magnitude. So, a snubber design based on the 1% is hardly ever useful [16].

The primary leakage inductance of flyback transformer has to be measured, by short circuiting the secondary during the measurement. The value of the parameter at the used transformer is  $65.8 \mu\text{H}$ . Another parameter needed is the ringing frequency, which is obtained from measuring the turn-off waveform at the oscilloscope. It should be two orders of magnitude higher than the switching frequency. If it is not the case, the dissipation will become excessive, so, the leakage inductance, the circuit capacitance, or both have to be reduced. The frequency is 3.85 MHz ( $T=256 \text{ ns}$ ) and

it meets the criteria.

The characteristic impedance of the resonant circuit has to be calculated by following the equation 3.20.

$$Z = 2\pi f_r L = 1572.37 \Omega \quad (3.20)$$

where  $f_r$  is the ringing frequency and  $L$  is the leakage inductance of the transformer.

The snubber resistor, which corresponds to the one in figure 3-6, has the same value of the characteristic impedance,  $R=Z$ .

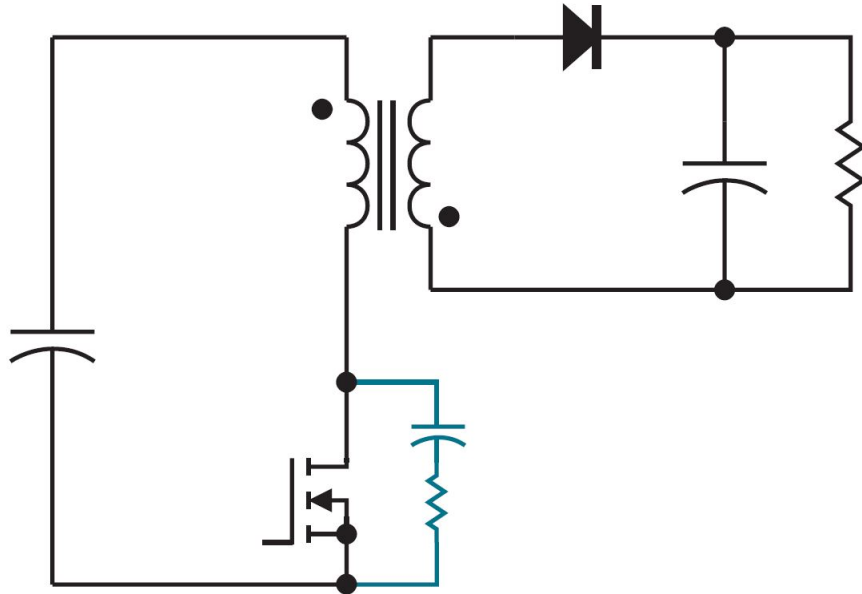


Figure 3-6: RC snubber circuit[16].

Regarding the snubber capacitor, it is used to minimize the dissipation at the switching frequency, so the best point to start is the one where the impedance of the capacitor is equal to the resistor, as the equation 3.21 shows:

$$C = \frac{1}{2\pi f_r R} = 26.3 \text{ pF} \quad (3.21)$$

As it is said above, the dissipation is determined by the the size of the snubber capacitor (equation 3.22)

$$P_{sn} = CV^2 f_s = 0.633 W \quad (3.22)$$

where  $V$  is the sum of the input voltage and the reflected output voltage, and  $f_s$  is the typical switching frequency of the TNY264GN (132 kHz).

Although removing the first peak is quite difficult, the oscillations are reduced which involves an EMI reduction. This first peak is very dangerous for off-line solutions using integrated power controllers so, it is necessary to clamp this voltage value to prevent the failure of the FET. Other circuits like RCD clamp or the TVS diode are used for this purpose.

The table 3.4 shows the values of the two prototypes.

Table 3.4: RC snubber values of PCB 1 and PCB 2

	Resonant freq.	Primary Ind.	Leakage Ind.	Z	C
<b>PCB 1</b>	3.85 MHz	534 $\mu$ H	65.8 $\mu$ H	1572 $\Omega$	26.3 pF
<b>PCB 2</b>	4.46 MHz	460 $\mu$ H	44.5 $\mu$ H	1247 $\Omega$	28.62 pF

At the second case, there was only available a capacitor of 22 pF, so the impedance was recalculated to fulfil the resonance calculation, so, the new impedance is 1620  $\Omega$ . Three resistances of 390  $\Omega$  and one of 470  $\Omega$  are chosen.

### 3.3.2 Primary RCD clamp

As it is known, this circuit is used to limit peak drain voltage to prevent switch over-voltage. It works absorbing current in the leakage inductor once the drain voltage exceeds the clamp capacitor voltage. The figure 3-7 shows the typical scheme.

First of all, the leakage inductance of the flyback transformer, which is measured in the previous part. The difference is that, now, the design is more concerned about how much energy is stored in the leakage inductance rather than the incremental leakage value for the ringing frequency.

Looking at the specifications of how much voltage can be tolerated by the power MOSFET, the peak clamp voltage is determined. The energy stored in the leakage inductance with a current  $I_p$  at the turn-off and, particularly, the power delivered

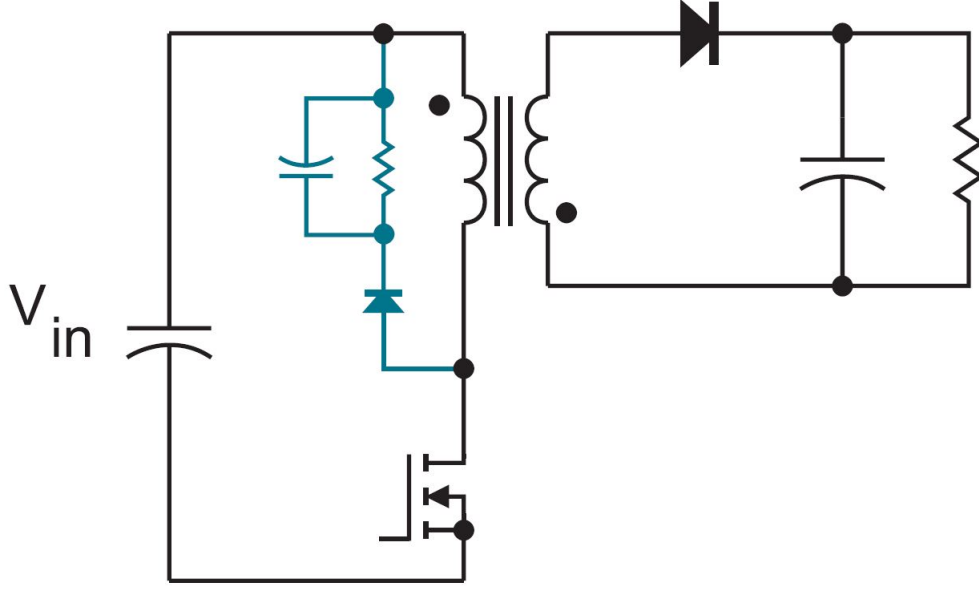


Figure 3-7: RCD clamp circuit[16].

is calculated in equation 3.23 where  $I_p$  is the peak limit current of the TNY264GN, 0.267 A

$$P_{Llk} = \frac{1}{2} L_{lk} I_p^2 f_s = 0.31 \text{ W} \quad (3.23)$$

Thus, the RCD clamp power delivered by the leakage inductance is expressed in equation 3.24, which denotes that the higher the clamp voltage rise, the lower the overall dissipation. So, this must be balance the total voltage across the power switch. The figure 3-8 shows the typical simplified waveform of the drain to source voltage. The values for the output reflected voltage and the maximum peak voltage are 28.44 V (previously calculated) and 100 V respectively. In order to adjust more the clamping voltage, a higher value of  $V_{x_{max}}$  can be chosen.

$$P_{sn}^{max} = P_{Llk} \left( 1 + \frac{V_{or}}{V_{x_{max}}} \right) = 0.398 \text{ W} \quad (3.24)$$

The capacitor is large enough that does not change its value while absorbing leakage energy. In any case, the value is not critical and it will not affect to the voltage peak. However, the resistor is crucial (equation 3.25) because the larger value, the

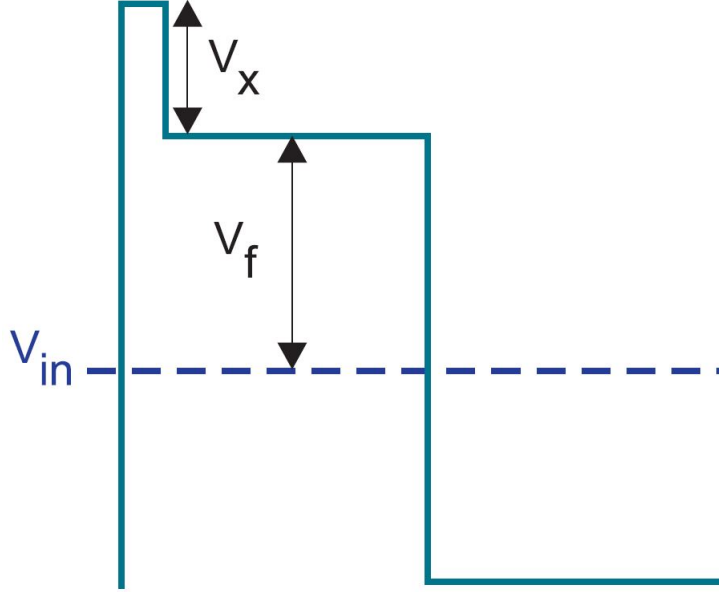


Figure 3-8: Typical waveform of drain-to-source voltage at turn-off[16].

slower discharge of the capacitor, so, voltage can rise higher value. But, the smaller the value, the lower clamp voltage and, so, the dissipation will be increased. The switching period is  $7.57 \mu\text{s}$  and  $V_x$  is  $100 \text{ V}$ .

$$R = \frac{2V_x T_s (V_{or} + V_{x_{max}})}{L_{lk} I_p^2} = 41.49 \text{ k}\Omega \quad (3.25)$$

The power losses of a known RCD clamp 3.27 for a given current peak and a leakage inductance. The value for  $V_x$  above the flyback voltage is given by the equation 3.26. It is supposed a resistance of  $36.4 \text{ k}\Omega$

$$V_x = \frac{1}{2} \left( \sqrt{V_{or}^2 + 2 \frac{L_{lk} I_p^2 R}{T_s}} - V_{or} \right) = 92.885 \text{ V} \quad (3.26)$$

$$P_{sn} = \frac{(V_x + V_{or})^2}{R} = 0.355 \text{ W} \quad (3.27)$$

There is a limitation for the RCD clamp. After clamping period is finished, the circuit resumes the ringing. Not with ideal components but, in reality, the diode of RCD has finite Reverse Recovery Time ( $t_{rr}$ ) which allows leakage current to flow in the opposite direction through the diode resulting in the ringing. The diode type is

crucial. It must be as fast as possible along with the power voltage rating.

The higher you allow the voltage to rise, the lower dissipation will take place but the voltage applied to the diode will increase a lot. It involves a more severe ringing, so, the EMI problem is not solved. This ringing can be damping by combination of the RC snubber, achieving the best protection of the MOSFET, the lowest EMI problems but the highest power dissipation.

### 3.3.3 Transient voltage suppressor (TVS) diode

This circuitry could be a valid substitute for the RCD clamping protection explained above. The performance of this solution is developed in this section along with the proper calculation for our case and finally, a decision between both options is made depending on the characteristics and priorities of our system.

A TVS diode or Transil, which is the trademark of ST Microelectronics, is an avalanche diode designed to clamp over voltages and dissipate high transient power[6].

A Transil has to be selected in two steps:

- Check that the circuit operating conditions do not exceed the specified limit of the component for non-repetitive surge operation, for repetitive surge operation and for normal operation.
- Check that the maximum value of the clamped voltage under the worst conditions corresponds to the specification of the circuit.

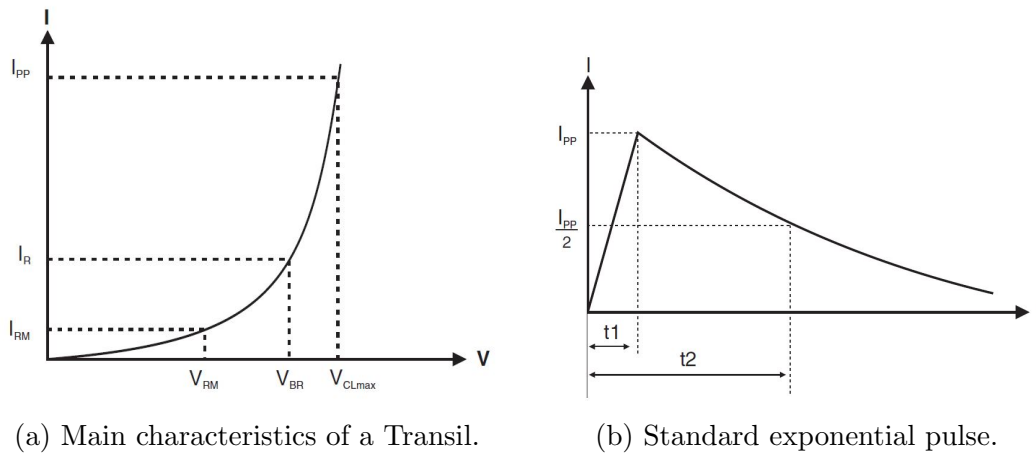


Figure 3-9: Transil performance curves[6]

Figure 3-9a shows different voltages of the Transil.  $V_{RM}$  is the voltage that the TVS can withstand in normal operation,  $V_{BR}$ , called breakdown voltage, is the voltage above which the current increases very fast for a slight increase in voltage and finally, the  $V_{CL}$ , clamping voltage, is the maximum value for a standard current pulse with a peak value. The clamping factor  $V_{CL}/V_{BR}$  characterizes the degree of protection. The figure 3-9b represents the most of standards used for protection devices. The performance of the Transil is given in the datasheet for both 8/20  $\mu s$  and 10/1000  $\mu s$  waves (t1/t2).

An important issue is the peak power dissipation of the Transil. As one of its objectives is to protect equipment against transient disturbances,so, by means of the curve peak pulse power vs pulse duration (figure 3-10) the right Transil could be chosen depending on the application. The average power dissipation is calculated by using of the equation 3.28 (in repetitive operation) where f is the switching frequency and the W is the energy dissipated at each pulse (energy stored in leakage inductor):

$$P_{AV} = f \cdot W = f \cdot \frac{1}{2} \cdot L_{lk} \cdot I^2 = 0.206 W \quad (3.28)$$

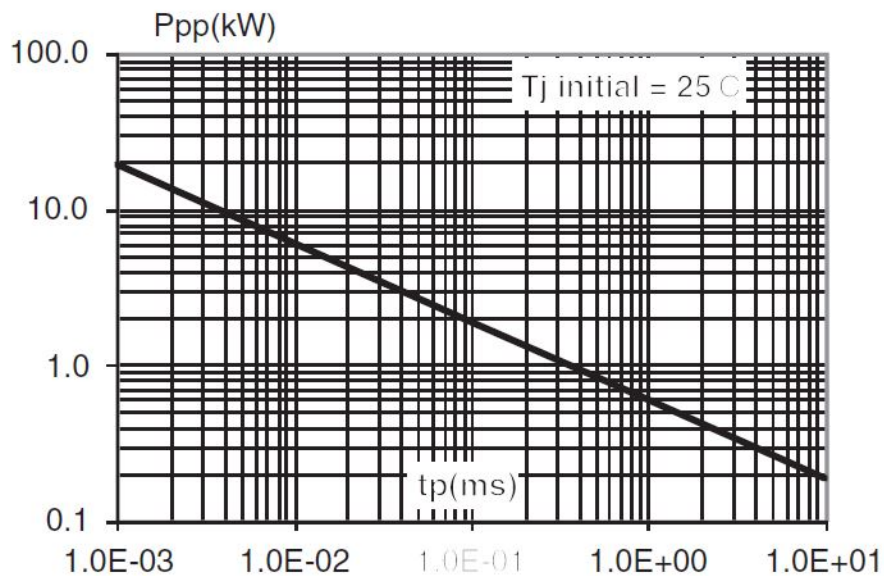


Figure 3-10: Peak pulse power vs exponential pulse duration curve[6].

The junction temperature is calculated following the equation 3.29 from the ther-

mal resistance and the power dissipation value (calculated before) and it should never exceed the maximum junction temperature established by the component.

$$T_j = T_{amb} + R_{Th_{j-a}} \cdot P_{AV} \quad (3.29)$$

Once a particular component is chosen, its thermal resistance will allow to calculate the junction temperature to check if it is suitable for our application.

Looking at the power losses, the TVS has a lower value than the RCD clamp circuit, as it is expected, due to the fact that the TVS only dissipates power when it clamps the voltage. However, the RCD clamp is an arrangement of more components and is consuming power during the whole switching period. Moreover, the TVS takes up less space than the RCD clamp, which is one of the most important requirements of our system.

## 3.4 Electromagnetic Interferences (EMI)

In this section, the possible electromagnetic interferences that take place in the system are described, the needed equipment for measuring these interferences, the types of noise produced by the power supply and some solutions are explained. From that point, the chosen solution is presented. Then, few sections below the results of the measurements before and after addressing this issue are analysed and compared.

### 3.4.1 Types of EMI

There are two main types of EMI in power supplies. The new SMPS have increased significantly the commutation frequency of the switches, leading to a faster rise and fall times for the voltage and the current than old power supplies. A faster switching reduces the losses a lot, improving the efficiency of the device. However, a high frequency lead to an interaction with the smaller passive components or also with the parasitic elements of them. So, the EMI performance is a very important part of the design and hast to be considered from the beginning[11], like reliability and safety.

Three things cause EMI problem:

- A signal source that creates some kind of noise.
- There is a transmission path for the noise.
- There is a sensitive receiver that can be distorted by the noise.

In our case, the most relevant causes are the generation of noise and the transmission paths of the PCB. The design must pass EMI testing and, also, it will work properly with good efficiency without being disturbed by other equipment. Although a power supply for a smoke detector is not usually installed in noisy environments, it will be tested in any case.

### 3.4.2 Measuring Conducted Emissions

Although there several EMI regulations, all of them are based in the same general concept. Conducted emissions are measured with a Line Impedance Stabilization Network (LISN)[5]. The figure 3-11 shows the filter  $L_F/C_F$  inside the device that allows the line frequency to flow but not the higher frequencies that flow the coupling capacitor  $C_C$  and the sense resistor  $R_S$ . An spectrum analyser receive the current emission signal as sensed voltages  $V_{SL}$  and  $V_{SN}$  in  $\text{dB}\mu\text{V}$ .

Conducted emission currents can flow to the AC mains only during the bridge rectifier conduction time which defines a “gating pulse” with “pulse repetitive frequency” (PRF) equal to the line frequency (50 or 60 Hz).

Normally, the spectrum analyser has a frequency range from 10 kHz to 1 GHz, and it displays the RMS value of the signal. For instance, for a 100 kHz continuous sinusoidal voltage of 1  $V_{peak}$  (0.7071  $V_{RMS}$ ). The spectrum analyser with has an input resistance of 50  $\Omega$  will give the results in  $\text{dB}\mu\text{V}$  and  $\text{dBmW}$  represented by the equations 3.30 and 3.31 respectively.

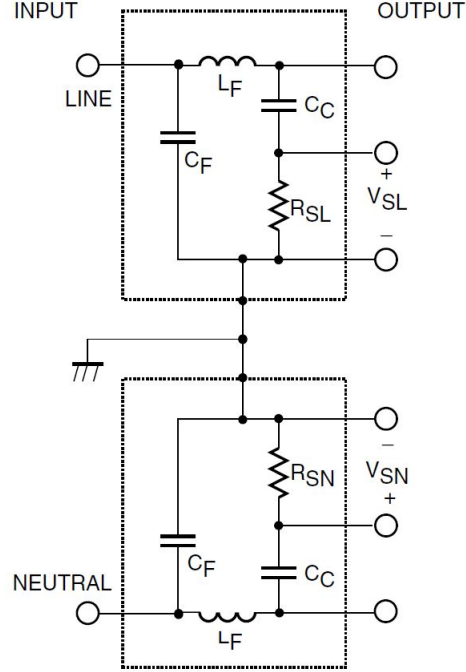


Figure 3-11: Line Impedance Stabilization Network (LISN)[5].

$$Amplitude(dB\mu V) = 20 \cdot \log \left( \frac{V_{RMS}}{1\mu V} \right) = 20 \cdot \log \left( \frac{0.7071 V}{1 \mu V} \right) = 117 dB\mu V \quad (3.30)$$

$$Amplitude(dBmW) = 10 \cdot \log \left( \frac{\frac{V_{RMS}^2}{R_{INPUT}}}{1 mW} \right) = 10 \cdot \log \left( \frac{\frac{0.7071^2 V}{50 \Omega}}{1 mW} \right) = 10 dBmW \quad (3.31)$$

Peak detection is the simplest and fastest method for measuring conducted emissions. From 10 kHz to 150 kHz measurements the resolution bandwidth is 200 Hz and, from 150 kHz to 30 MHz the resolution is 9 kHz. The peaks are not constant but change in magnitude. Many spectrum analysers have a “maximum hold” feature which displays the highest peak over all the measurements. The average detector is simply a low pass filter with corner frequency sufficiently below the gating pulse repetitive frequency. Another type of measurement is the quasi-peak detector which is designed to indicate the subjective annoyance level of interferences. It means that

the soft noise produced every second is much more annoying than the loud noise produced every hour. So quasi-peak detector behaves as a leaky peak detector that partially discharges between input signal pulses[5]. If a peak detector meets the average specification with an additional margin any more measurements are needed.

### 3.4.3 Types of noise

One important differentiation is the one between common and differential noise. Common noise is caused by a capacitive coupling of the switching stage into ground and appears with the same phase and amplitude in both lines[11]. Differential noise is caused by the time-varying current demands of the switching stage.

#### Differential mode noise

This type of noise is conducted on the signal (VCC) line and ground (GND) line in the opposite direction to each other. Figure 3-12 shows the differential noise current path.

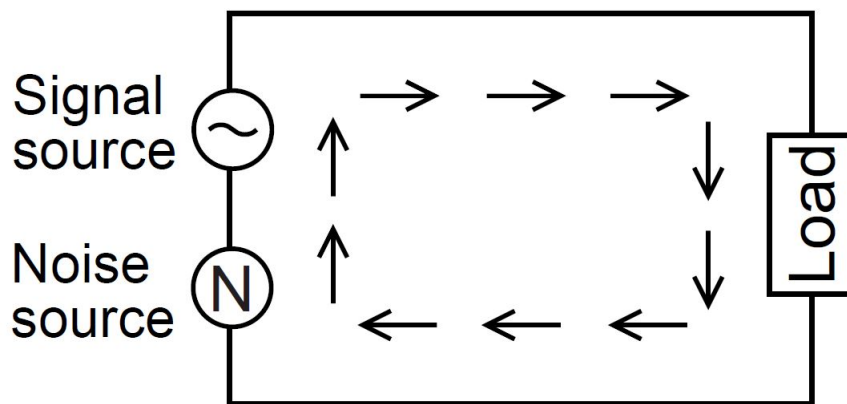


Figure 3-12: Differential mode noise transmission path[2].

This noise is produced mainly by the interaction between the parasitic elements of the DC blocking capacitor (typically electrolytic) and the high frequencies of the commutation. Figure 3-13 represents a comparison between ideal and real capacitors. As it can be seen the impedance decreases with the frequency. But, due to the parasitic resistance (ESR) and inductance (ESL) elements it will behave differently

from the ideal situation. The ESL creates a capacitor resonant frequency, which is determined by the ESR of the capacitor. Beyond this frequency, the capacitor behaves as an inductor[5].

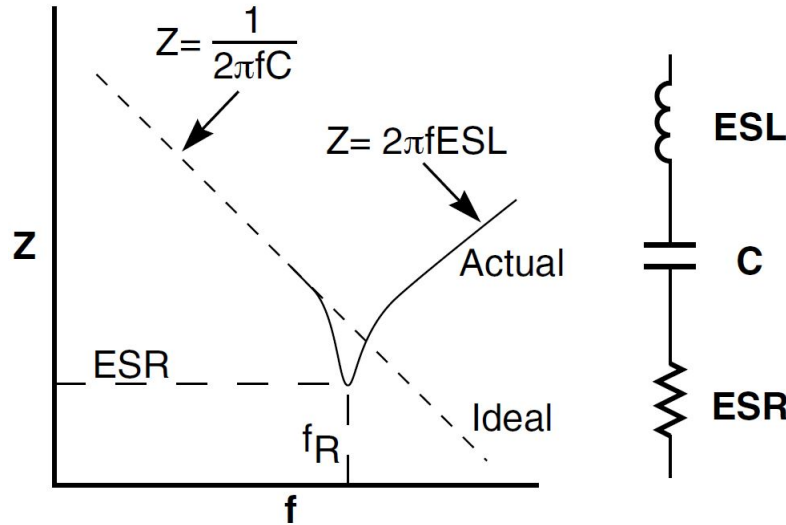


Figure 3-13: Comparison between ideal and real capacitors[5].

To counteract this differential mode noise some capacitors for suppression of interferences and safety recognized are widely used and they divided in two groups, X and Y capacitors. X-capacitors, only used in positions where its failure does not expose anybody to an electric shock hazard, are usually connected across the AC mains, and particularly, X2-capacitors are commonly used as a EMI filter for differential mode suppression. Y-capacitors, which have the function of isolating when its failure could expose somebody to an electric shock hazard, are usually connected between both sides of the power supply transformer.

There are also many filter topologies to address differential noise, the basic ones are described below in figure 3-14.

Depending on the required attenuation, the filter needs to have one, two or even three stages. The best form factor is achieved with a balanced implementation, making the filter long and thin reducing the coupling capacitance and increasing the impedance between input and output. The PI filter is the most commonly used and it works very well in most of SMPS due to connection of the large bus capacitor at the output of the filter. The T filter has an inductive input and output, and its input

Schematic	Loss per octave
<b>pi filter</b>	
	18 dB / oct
<b>T filter</b>	
	18 dB / oct
<b>L filter</b>	
	12 dB / oct

Figure 3-14: Types of basic input filters [11]

makes life easier for over-voltage protection at the input [11]. For difficult lines it would be the best option. The L filter only has 12 dB of attenuation per octave since it has two elements, so a double-L may be needed. In this case, the output capacitor cannot replace the filter output capacitor because its self-resonant frequency is very low.

### Common mode noise

The common mode noise is conducted on all lines in the same direction (figure 3-15). The coupling capacitance which produces this type of noise is very small, so the line-to-line capacitors and the small inductors of the differential mode noise filters are not valid.

The typical points where the common mode noise is generated are the drain-to-heatsink capacitance and also the transformer interwinding capacitance. The last causes currents to flow between the isolated (primary and secondary) sides of the

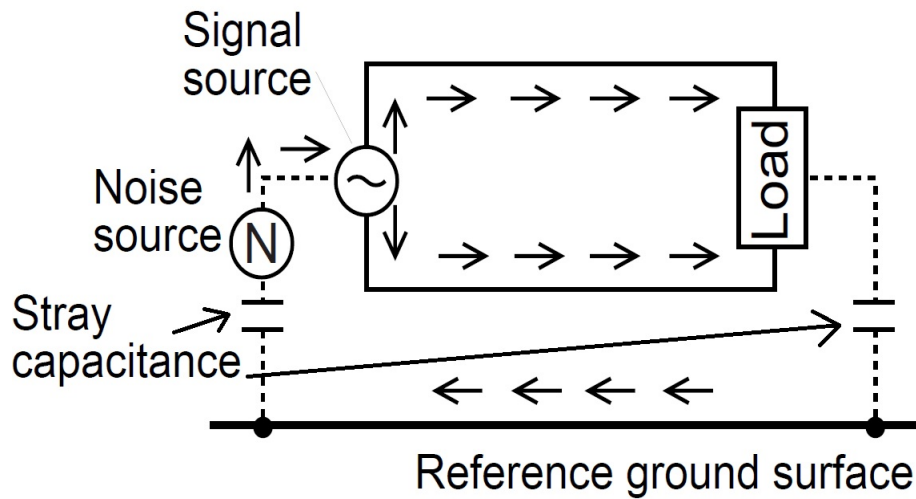


Figure 3-15: Common mode noise transmission path[2].

transformer, and can produce a high-frequency component at the secondary [9]. A solution could be a Y-capacitor (explained above) connected between primary and secondary grounds, and another effective solution is the use of a “common mode choke” that consists in two inductors wound in the same core in such a way that the magnetic fields caused by differential mode currents are cancelled [5]. Figure 3-16 shows a toroidal implementation which is not always the best option for low cost and practical EMI filter. An important advantage of the common mode choke is its inherent differential mode choke, so any other is needed.

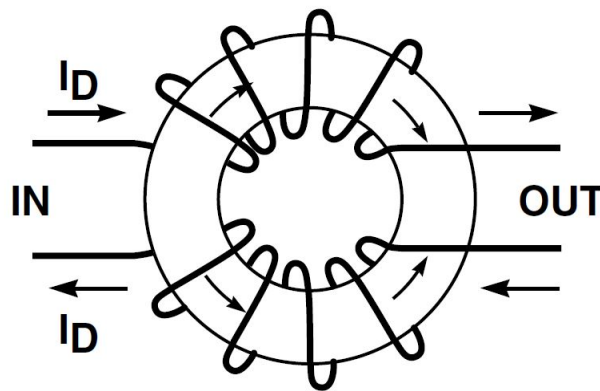


Figure 3-16: Typical common mode choke[5].

### 3.4.4 Study of our system

The first adopted solution is to add a Y-capacitor between one of the primary terminals and one of the secondary terminals of the transformer. There are several options of placing the Y-capacitor, the datasheet of the TNY264GN advise to put it between the the positive primary terminal and the secondary ground terminal. This configuration is very suitable for filtering common mode noise, so it is the final solution. Afterwards, at the tests section, the complete description of the procedure and the different tested configurations are explained along with the measurements of the equipment used.

In terms of differential mode noise, the PI filter is the most common solution for SMPS. Thus, this configuration is designed for our particular case. First of all, the design impedance is calculated [11] in the equation 3.32, from the minimum voltage at the primary,  $V_{min}$ , and the maximum current,  $I_{max}$ :

$$Z_d = \frac{V_{min}}{I_{max}} = \frac{95.94 V}{300 mA} = 319.8 \Omega \quad (3.32)$$

The filter cut-off frequency is determined from the attenuation of the frequency problem, while at the same time producing a minimal attenuation at the line frequency. So, the cut-off frequency should be placed a decade below the switching frequency,  $f_{cut} = 13.2 kHz$ . The inductance and the capacitance are calculated in equations 3.33 and 3.34.

$$L = \frac{Z_d}{2\pi f_{cut}} = 3.846 mH \quad (3.33)$$

$$C = \frac{1}{2\pi f_{cut} Z_d} = 37.7 nF \quad (3.34)$$

Then, the capacitance can be divided by two in order to built the proper PI configuration. Once, the prototype is tested in the LISN, different configurations are tried in order to get a good performance



# Chapter 4

## Simulation

In this section, a simulation is carried out for analysing in a different way the performance of the system by using PSIM. It is important taken into account that this simulation does not model exactly the operation of the TinySwitch but it intended to be a close one. The component models are far from the reality but, at this level of simulation, they are enough for taking some numbers before building the PCB. An open-loop simulation is developed to obtain some waveforms, measurements of the input and output voltage and current ripples and the maximum values of specific variables.

Some components calculated in the previous are used for the simulation but in the case of the flyback transformer the values of the component made in the laboratory are used instead of the theoretical ones.

In this simulation another component is added at the end in order to make a closer situation to the reality and to compare the effects of having it. It is the leakage inductance of the flyback transformer.

The figure 4-1 represents the open-loop simulation scheme from the grid to the load. The voltage grid is set at the maximum value for which the power converter is designed,  $265 V_{AC}$ , to measure the peak voltage at the MOSFET during the turn-off and the maximum current values of the whole circuit. Any auxiliary circuits are not taken into account in this first simulation because the main performance of the system is not affected by them. However, the clamping circuit is added afterwards to

see how it limits the  $V_{CE}$  voltage of the MOSFET during the turn-off.

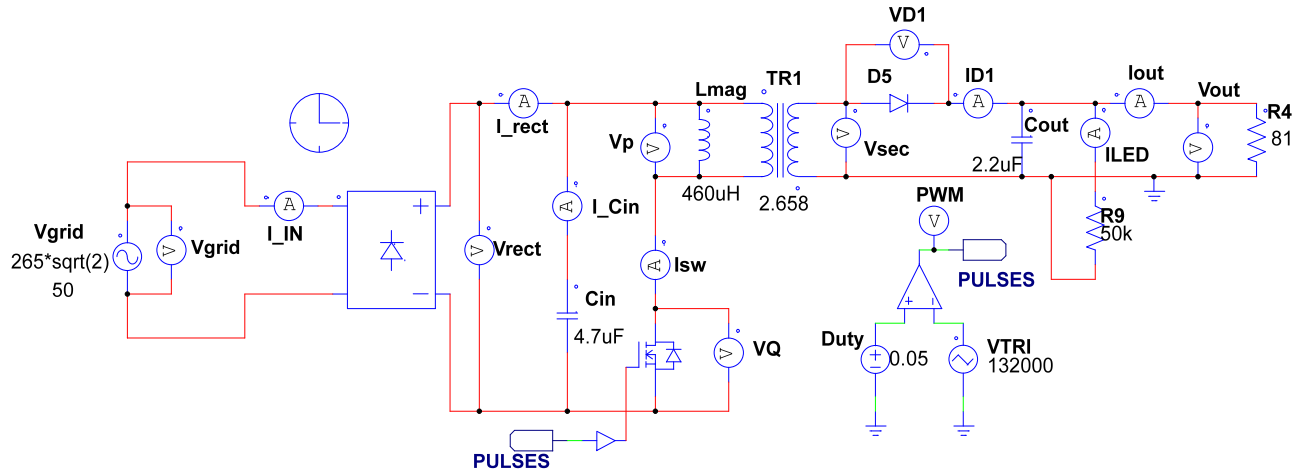


Figure 4-1: Open-loop simulation scheme

It is easy to appreciate in figure 4-2 the input voltage ripple of 15.26 V and also the conduction of the rectifier diodes while the input capacitor is charging. The duty is fixed at 0.05, so the average output voltage is around 14 V. By carrying out a better adjustment of the duty, it would be easy to obtain the 9 V. The output voltage has a low frequency ripple that comes from the input capacitor and a high frequency ripple at the commutation frequency.

The figure 4-3 shows the different switching variables where the different states of the DCM operation are easily appreciated. During the ON-state, the current through the MOSFET reaches 0.295 A and transfers the energy to the magnetizing inductance. As it is expected, the difference between the secondary voltage and the output diode voltage is the value of the output voltage. At the turn-off, the MOSFET withstand 412 V and the energy starts to be transferred to the secondary side. The primary side voltage changes its polarity, and the output diode conducts with a voltage drop of 1 V across it.

When the current through the diode reaches zero, the voltage at both sides of the transformers becomes zero, so the voltage at the output diode is the same as the output voltage. The current is also zero through the MOSFET and the output diode. During this sub-period the MOSFET withstands the rectified grid voltage.

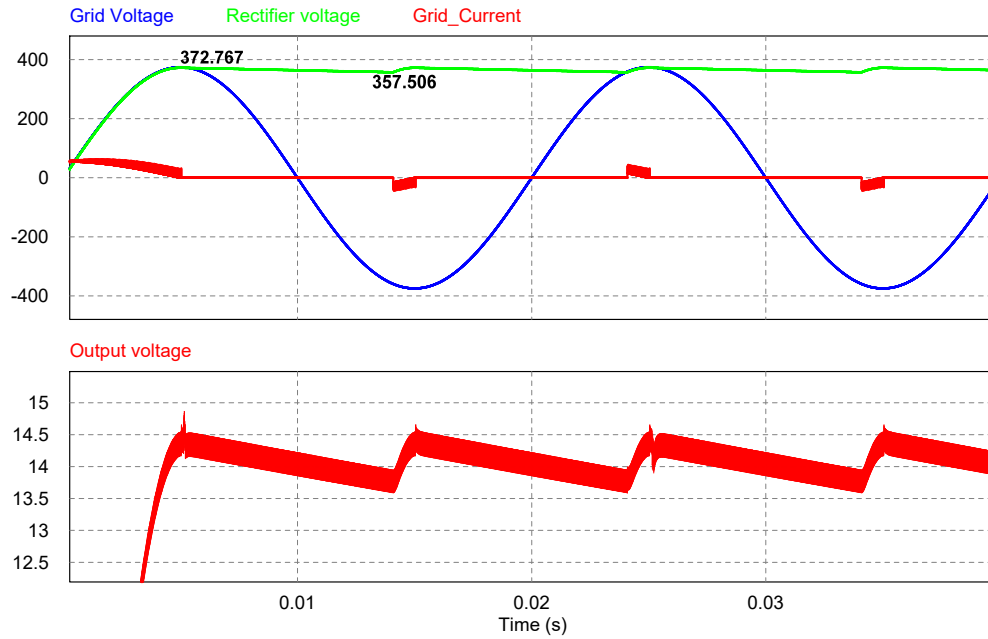


Figure 4-2: Input voltage/current and output voltage

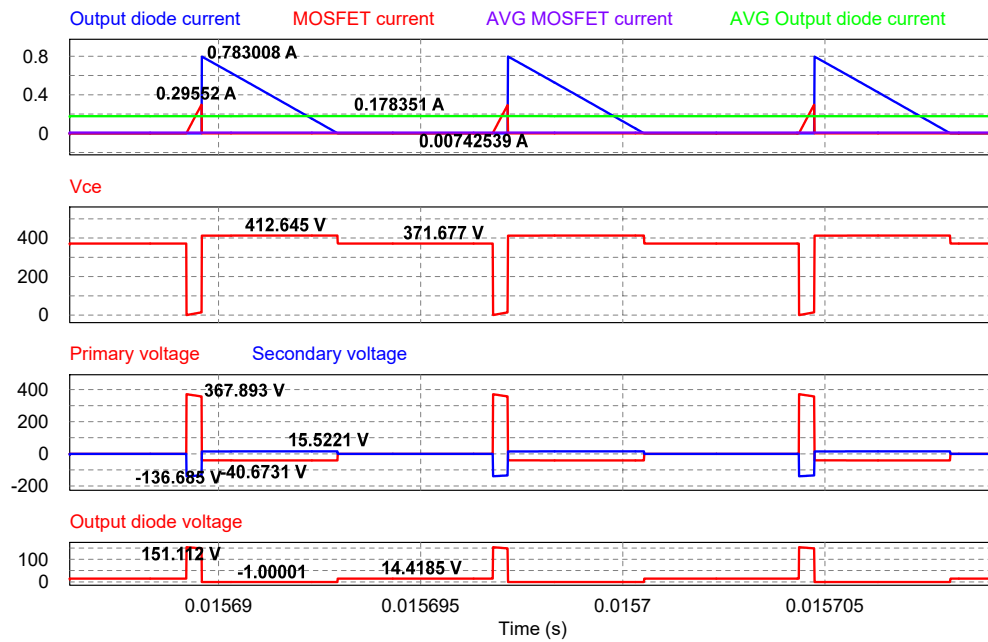


Figure 4-3: Switching variables

The average current values are also represented and this important information is taken into account for the component selection in terms of the effective current that a specific component has to withstand.

Looking at the figure 4-4 shows the output variables to observe the voltage and current ripple. The low frequency voltage ripple is around 0.8 V and in terms of current is 12 mA. This ripple is directly related to the input capacitor. The high frequency voltage ripple that comes from the switching has a value of 0.3 V and 5 mA for the current ripple.

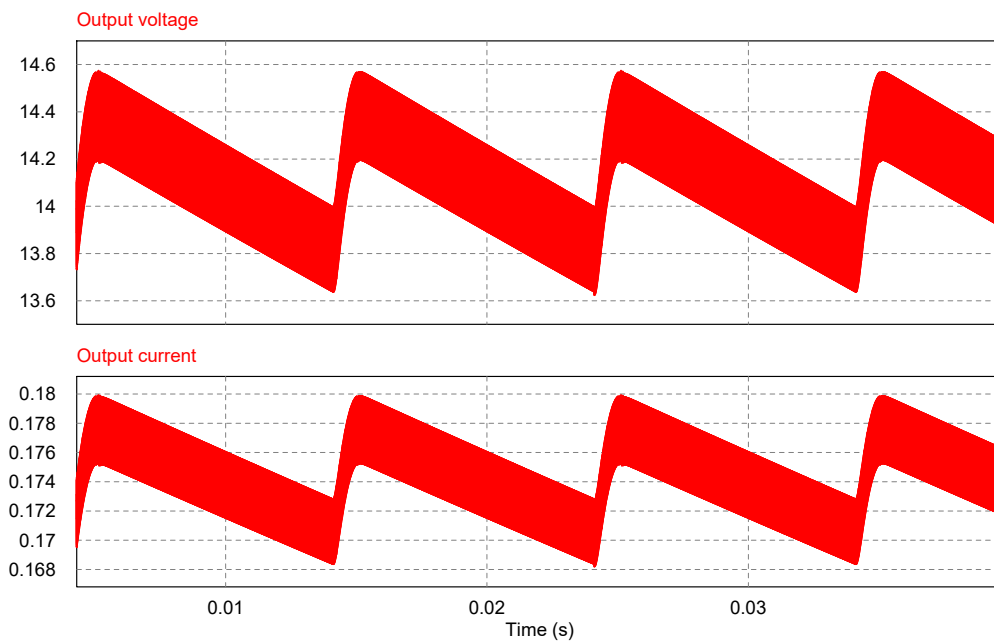


Figure 4-4: Open-loop output variables

The performance of the clamp circuit is also analysed in the open-loop simulation and as it can be seen a 160 V zener and a diode are placed and the leakage inductance of the flyback transformer which is directly related to the voltage peak at the turn-off of the MOSFET.

The clamping circuit is working properly as the figure 4-5 shows, because the voltage peak at the turn-off is limited by the 160 V zener. The voltage at zero conduction sub-period plus the zener breakdown voltage equals the voltage limit of the collector-emitter voltage, 532.7 V. Without this auxiliary circuit the peak would be higher and it could reach the MOSFET voltage limit, 700 V.

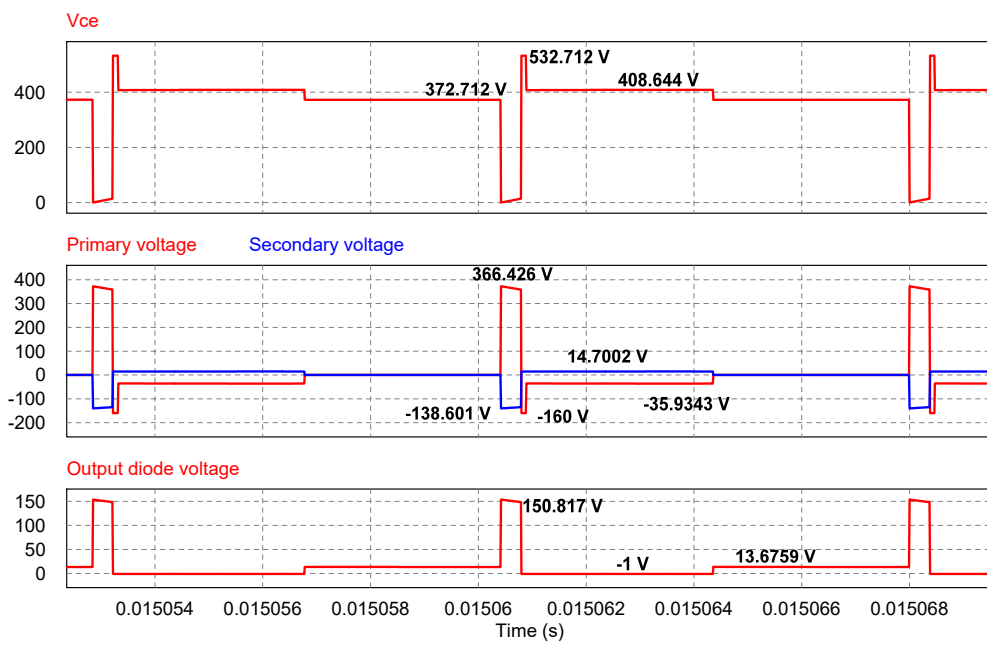


Figure 4-5: Clamping circuit open-loop curves



# Chapter 5

## Components selection

In this section, the selection of all the commercial components of the power supply is carried out regarding the price, the reliability, the size and the efficiency of each component. The reliability is especially critical in some key components like the electrolytic capacitors, so in this case, this feature has to be taken into account with the same importance than the size and the price. After the selection component by component paying attention to the their features and the circuit requirements a table with all the components is shown. The reference price for every component is the corresponding to the order with largest number of components, in particular for SMD components which are packaged in reels. NormaGrup Technology has an internal web site which is a database of all the components the company has. Thus, a requirement is the use of the components from this database.

### 5.1 Grid connection and rectifier

#### 5.1.1 Terminal block

The connection to the grid is a critical point due to isolation issues. The regulation UNE-EN 61558:2005, part 26 establishes the distances between active parts of the circuits. The pitch of the component is the distance between pins and in this case, a terminal block from TE Connectivity is chosen with a 5 mm of pitch. The fastening

of the cables to the terminal block is based in a simple screw. This component is chosen because it meet the criteria of the isolation regulations and has the minimum possible size for our PCB.

### 5.1.2 Grid fuse

The fuse which protects the whole circuit against short-circuits has to be selected. The rated values of voltage and current are  $265 V_{AC}$  and 1 A respectively. The fuse from AEM, MF2410F1.000TM ( $250 V_{AC}$ , 1A), is suitable for this case as it is the cheapest one.

### 5.1.3 Rectifier bridge

As it is calculated above, the rectified voltage is around 374 V, so a component with a DC blocking voltage of 400 V could be enough. However, looking at several manufacturers, a bridge rectifiers from Diodes Integrated is chosen due to its price and higher DC blocking voltage, 600 V. The average rectified current for this component is 0.8, which is an acceptable value for the current levels of this prototype.

## 5.2 EMI input filter

The EMI input filter calculated at the end of chapter 3 is composed of an inductor and two film capacitors. Starting from the inductor, there are a lot of commercial valid components but an axial one from Abracon LLC is chosen because it has a good price. The value of the inductance, 3.9 mH, is higher than the calculated one, 3.8 mH, but the only consequence is the decrease of the cut-off frequency up to 480 Hz which a suitable value.

The capacitor of the filter has a value of 33 nF, the final decision is to divide the value of the capacitance between two capacitors, but not equally, the first capacitor has lower value than the second one. This configuration improves the dynamic performance of the PI filter. The first capacitor is a film capacitor of 1.8 nF, with 400 V

of rated voltage from Arcotronics. The second capacitor has a capacitance of 27 nF from Faratronic.

### 5.3 Input capacitor

The input capacitor along with the output one, are electrolytic capacitors due to the necessity of filtering the voltage ripple at the input (produced by the rectifier bridge) and the voltage ripple at the output (produced by the commutation of the MOSFET and the flyback).

As it is widely known, the electrolytic capacitors are the critical components of any power electronics device because of its short-life in comparison with the rest of the components, so, the choice of a suitable electrolytic capacitor make the difference between a long-lasting device or the opposite case. The key parameters that have to be taken into account are the maximum voltage the capacitor can withstand, the maximum current ripple through it and the operation temperature of the system.

The ripple current heats the capacitor and the maximum permitted ripple current is set by how much can be permitted and still meet the capacitor's load life specification[1]. If the temperature of the capacitor's core rises, it can fail quickly, or by operating close to the maximum core temperature the life can be shorted. Normally, the load life at maximum core temperature is between 1000 and 10000 hours. As it is known the power dissipated is the current ripple squared times the ESR. Since ESR decreases at high temperatures, less than the maximum ESR can be used to calculate the power dissipation.

An important parameter is the dissipation factor, which is the measurement of the tangent of loss angle ( $\tan \delta$ ) expressed as percentage. It is also the ratio of the ESR to the capacitive reactance and follows the equation 5.1, where  $f$  is Hz,  $C$  in  $\mu\text{F}$  and ESR in  $\Omega$ . As the data-sheet usually gives the DF (Dissipation Factor) parameter, it is easy to obtain the ESR, and then, the power dissipated is calculated straightforward.

$$DF = \frac{2\pi f C (ESR)}{10000} \quad (5.1)$$

A 4.7  $\mu\text{F}$  400 V capacitor is chosen for the input to obtain a voltage ripple around 10-20 V. It has a maximum ripple current of 42 mA at 120 Hz and 105°. The rated power of the system is 1 W so any inconvenient in terms of heat is taken into account.

The ripple temperature multiplier calculated in the equation 5.2, takes into account the ambient temperature ( $T_a$ ), the rated temperature ( $T_r$ ) specified in the data-sheet and the maximum core temperature ( $T_c$ ) which is always higher than the rated temperature. If the capacitor is large enough, there is a 5°C from the surface to the can, and another 5°C from the can to the innards, so 10°C of difference can take place[13]. However, this input capacitor size is not too large, so it is supposed a difference of 2 degrees from the surface of the capacitor to the core. This temperature multiplier is calculated with an ambient temperature of 20°C because the device will usually be inside a room in a building.

$$\text{RippleTemperatureMultiplier} = \sqrt{\frac{T_c - T_a}{T_c - T_r}} = \sqrt{\frac{107 - 20}{107 - 105}} = 6.6 \quad (5.2)$$

The rated ripple current is adjusted for operation at 120 HZ, but if the frequency increases. Even so, it is difficult to make tables that accurately model the dependence of this two parameters. The data-sheet of the chosen capacitor does not show this table, but looking for specifications of similar capacitors in terms of capacitance, rated voltage and rated ripple current, a suitable frequency multiplier for 100 kHz can be 1.6. Therefore, the equation 5.3 shows the adjusted maximum ripple current for this particular case.

$$\text{MaxRippleCurrent} = 42 \text{ mA} \cdot 6.6 \cdot 1.6 = 443 \text{ mA} \quad (5.3)$$

This maximum current ripple is high enough to work always below it. Thus, the 4.7  $\mu\text{F}$ , capacitor from Capxon is appropriate for the application.

## 5.4 RC snubber and clamp circuit

The components for the auxiliary circuits are chosen in this section.

### 5.4.1 RC snubber

As it is calculated above, the resistance is  $1640\ \Omega$  but it is necessary to divide this total resistance among 4 individual resistors to withstand the applied voltage that a 0805 package cannot withstand (not higher than 150 V). They are from Yageo, three  $390\ \Omega$  and one  $470\ \Omega$ . Regarding the snubber capacitor a ceramic one of 22 pF (0805) from Samsung Electro-Mechanics.

### 5.4.2 Clamping circuit

Although, in this circuit is intended to use a transient voltage suppressor but a zener diode has the same performance at these voltage levels keeping them inside the limits, so the clamping function is really assured. This zener, from On Semiconductors, has a voltage range from 3.3 V to 200 V and a ESD rating of Class 3. The zener has to dissipate a power of 0.206 W according to the calculation made in previous chapter, so the chosen one is suitable because it can dissipate up to 550 mW in steady state. Particularly, the model is the 1SMB5954BT3G which has a zener voltage of 160 V. The clamping circuit diode has to be a FAST diode, so the US1J which is an ultra-fast, cheap and robust diode with a peak repetitive reverse voltage of 600 V is selected for this purpose. Moreover, both the average rectified output current and the peak forward surge current of the device, fulfil the needs of the system.

## 5.5 TinySwitch

The Tiny is the TNY264G, it has more power capability than the one needed for this particular system but as it is used in most of company products so, it is selected to avoid the costs of buying a different integrated circuit. Moreover, although the TNY264G (5 W) is oversized in terms of power for this system, the results are well

enough to not have the necessity of changing the model. The bypass capacitor used in the internal power supply of the TNY264GN is a  $0.1\mu\text{F}$  ceramic one from AVX. The EN/UV pin resistance, which has the function of enabling the TinySwitch depending the line voltage, is divided in 4 resistances of  $680\text{ k}\Omega$  to share the line voltage because the 0805 package does not withstand more than  $150\text{ V}$ . Thus, Yageo is the chosen manufacturer for this components. The EN/UV pin resistance at the first prototype was  $2.7\text{ M}\Omega$  but with this value, the minimum working voltage is shown in equation 5.4.

$$V_{min} = 49\ \mu\text{A} \cdot 2.7\text{M}\Omega = 132.2\text{V} \Rightarrow V_{AC_{min}} = 93.557\text{ V} \quad (5.4)$$

To make the TinySwitch work at  $85\text{ V}_{AC}$  it is necessary to reduce the resistance as it can be seen in the equation 5.5.

$$V_{min} = 85\sqrt{2} = 120.21\text{ V} \Rightarrow R = \frac{120.21\text{ V}}{49\ \mu\text{A}} = 2.45\text{ M}\Omega \quad (5.5)$$

Therefore, changing the value of one of the four resistors to  $330\text{ k}\Omega$ , a total resistance of  $2.37\text{ M}\Omega$ . The voltage drop in every resistor is inside the limits of the package.

## 5.6 Flyback transformer and decoupling capacitor

### 5.6.1 Flyback transformer

Once the flyback transformer is designed and its parameters are calculated, a prototype is built in the laboratory as it is explained in the previous chapter. Different configurations are made using horizontal and vertical coil formers, but finally a vertical one is chosen to take up less space than the horizontal one. It is difficult to obtain the same values so, the parameters are sent to Tonwell, a manufacturer of magnetics components among others and they make the custom transformers for this particular case. The parameters, as it is said before, are the theoretical ones, this implies a future recalculation of the auxiliary circuits like the snubber but knowing

the procedure is straightforward.

## 5.6.2 Decoupling capacitor

As it is explained in chapter 3, the Y-capacitor connected through the transformer terminals have different functions like isolation and suppression of common mode noise. The chosen one is a ceramic disc capacitor from Vishay. It is a class X1, 440  $V_{AC}$  and class Y2, 300  $V_{AC}$  according to the IEC60384-14.4. It has a value of 2.2 nF and, due to the Y2 classification, it can withstand a surge voltage of 5 kV.

## 5.7 Output diode and capacitor

### 5.7.1 Output diode

A fast diode is also needed for a suitable DCM operation so the ultra-FAST used at the clamping circuit is selected because of its fast reverse recovery time, 75 ns. In terms of current and voltage ratings, it does not have any drawback. The US1J has 1 A of average rectified output current when and 30 A of peak forward surge current.

### 5.7.2 Output capacitor

As it is said above, the temperature, the voltage and the current ripple through the capacitor are the main parameters for choosing the right capacitor. First of all, our power supply has a rated power of 1 W, which implies that in normal conditions the reached temperature is very lower than the rated one. The component is from Jamicon, with a range voltage of  $-55^{\circ}C \sim +105^{\circ}C$ . The rated voltage is not a big deal either because a 50 V capacitor is chosen, the voltage margin is large enough.

However, it is necessary to study in detail the current ripple through the capacitor. Looking at the data-sheet, the maximum current ripple is 19 mA at  $105^{\circ}C$  and 120 Hz but in normal conditions the ripple frequency is 100 kHz and the ambient temperature is around  $20^{\circ}C$ . Thus, a correction has to be made to by using multipliers, which are usually shown in the specifications, to obtain a suitable maximum ripple current.

The ripple temperature multiplier calculated in the equation 5.6. This output capacitor size is very small, so it is supposed a difference of 1 degree from the surface of the capacitor to the core.

$$RippleTemperatureMultiplier = \sqrt{\frac{T_c - T_a}{T_c - T_r}} = \sqrt{\frac{106 - 20}{106 - 105}} = 9.27 \quad (5.6)$$

The rated current ripple is adjusted for operation at 120 HZ, but if the frequency increases more current ripple is allowed. The table of the data-sheet shows suitable frequency multiplier for 100 kHz can be 1.6. Therefore, the equation 5.7 shows the adjusted maximum ripple current for this particular case.

$$MaxRippleCurrent = 19 \text{ mA} \cdot 9.27 \cdot 1.7 = 299.42 \text{ mA} \quad (5.7)$$

From this calculation, it is concluded that the capacitor of 2.2  $\mu$ F from Jamicon is suitable because the maximum current ripple permitted is higher than the current ripple calculated in chapter 3.

## 5.8 Optocoupler and feedback circuit

The optocoupler, key component of the feedback loop, is the HCPL-181. It has a competitive price, and low-forward voltage (1.2 V). Although, there are other components that withstand higher temperatures than 100°C, but it is a suitable maximum temperature because the prototype will not reach these levels. The voltage drop in the LED of the optocoupler involves the adequate choice of a zener diode as it is calculated, in the equation 5.8, with the maximum value regarding the datasheet, 1.4 V.

$$V_z = V_o - V_f = 9 \text{ V} - 1.4 \text{ V} = 7.6 \text{ V} \quad (5.8)$$

A zener diode from Vishay is chosen, the TZMC7V5-GS08, with a zener voltage

of 7.5 V. A current limitation through the optocoupler is needed so two resistors, one in parallel and another in series with the IC are connected. As the maximum average forward current is 50 mA, the series resistor has a value of 330  $\Omega$  that along with the 560 $\Omega$  parallel resistor to obtain a current of a around 30 mA when the zener conducts.

## 5.9 Output indication LED

The output indication LED lights when there is voltage at the secondary side. The chosen component is one from Lite-On, which has a maximum DC forward current of 30 mA so a resistor is needed in series to limit the current through the LED. A 39 k $\Omega$  resistor from Yageo is used.

## 5.10 Price of the prototype

The price of the system is estimated by searching the cheapest components that the main suppliers offer and by looking at NormaGrup database where every component used in the production is classified. The table 5.1 is a brief representation of all the components used in the prototype 2 along with the ID in the schematic, the manufacturer, the type of footprint, the unity price and the total price of the system which is 1.548 €. The unity prices are related to great orders of thousands of components as the company buy them.

Table 5.1: Price of the prototype 2

PCB ID	Component	Description	Manufacturer	Footprint	No.	Price	Total
C1	Cap 1,8 nF	Film capacitor PI filter	Arcotronics	Thr. hole	1	0,080 €	0,080 €
C2	Cap 27 nF	Film capacitor PI filter	Faratronic	Thr. hole	1	0,023 €	0,023 €
C3	Cap 4,7 uF	Input capacitor	Capxon	Thr. hole	1	0,066 €	0,066 €
C4	Cap 22pF (50VDC)	Capacitor for RC snubber	Samsung Electro-Mech	SMD	1	0,002 €	0,002 €
C5	Cer Cap 0,1uF	Capacitor ByPass Tiny	AVX	SMD	1	0,003 €	0,003 €
C6	Cap 2,2 nF 440 V	Capacitor Y2 EMI decoupling	Vishay	Thr. hole	1	0,054 €	0,054 €
C7	Cap 2,2 uF 35 V	Output capacitor	Jamicon	Thr. hole	1	0,011 €	0,011 €
D1	HD06	Rectifier Bridge	Diodes Integrated	SMD	1	0,043 €	0,043 €
D3, D2	US1J	Diode secondary winding, Clamping circuit diode	Diodes Integrated	SMD	2	0,029 €	0,057 €
DL1	LED Verde	LED ind. tensión secundario	Lite-On	SMD	1	0,011 €	0,011 €
DZ1	TZMC7V5-GS08	Zener diode feedback circuit	Vishay	SMD	1	0,010 €	0,010 €
DZ2	TVS clamp zener	Zener diode clamping circuit	On Semiconductor	SMD	1	0,065 €	0,065 €
F1	MF2410	Fusible entrada red	AEM	SMD	1	0,108 €	0,108 €
IC1	TNY264G	Tiny Converter	Power Integrations	SMD	1	0,439 €	0,439 €
IC2	HCPL-181-00BE	Optocoupler	Avago Technologies	SMD	1	0,117 €	0,117 €
L1	Inductor 3,9 mH	Inductor for PI filter	Abracon LLC	Thr. hole	1	0,084 €	0,084 €
R1,R2, R3, R4	Resis 390 (3) ohms 5% Resis 470 (1) ohms	Resistors of RC snubber	Yageo	SMD	4	0,002 €	0,008 €
R10	Resis 330 ohms	Resistor series Zener	Yageo	SMD	1	0,002 €	0,002 €
R11	Resis 39K	Resis for LED	Yageo	SMD	1	0,002 €	0,002 €
R5,R6,R7,R8	Resis 680K (3) 5% Resis 330K (1)	Resistor on EN pin	Yageo	SMD	4	0,002 €	0,008 €
R9	Resis 560 ohms	Resistor parallel Optocoupler	Yageo	SMD	1	0,002 €	0,002 €
TR1	Trafo E16/8/5	Flyback Trafo 460 uH	Tonwell	Thr. hole	1	0,230 €	0,230 €
X1, X2	Terminal Block 5mm	Grid Connector	Xinya	Thr. hole	2	0,061 €	0,122 €
							<b>1,548 €</b>

# Chapter 6

## Schematic, PCB design and final prototype

In this chapter, the schematic and the design of the PCB is explained. The needed changes due to the difficulties of prototyping and the components ratings are made. The standards and regulations related to the printed circuit boards are also taken into account and are well described.

### 6.1 Schematic design

The software used is Altium Designer. NormaGrup Technology S.A. which is a partnership during this project, has an Altium library with a great amount of components at schematic library as much as at the PCB library. The figure 6-1 corresponds to the second prototype created because several differences from the first one are noted like the PI filter, which was not taken into account; the clamping circuit, which in the first version was based in a RCD clamp, and also the values of the snubber and EN/UV pin resistances were changed to achieve a better adjustment of the circuit performance.

The schematic component of the TNY264GN is created by following the data-sheet of the component. The related pins of the flyback transformer are modified from an existent schematic to fit the right configuration. It should be pointed out



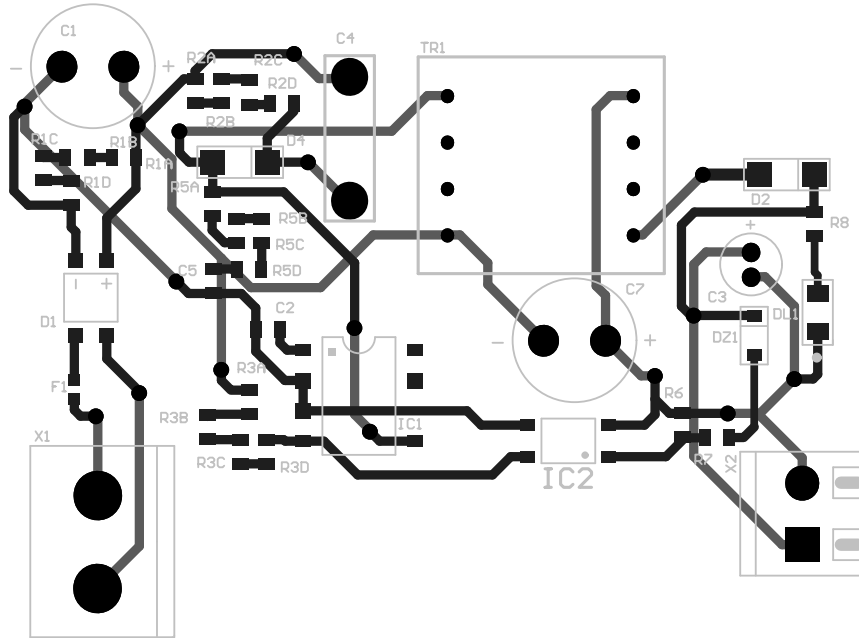


Figure 6-2: PCB 1

In the figure 6-2 both top and bottom layers are represented, the darkest tracks are from the top layer. As it can be seen the transformer has the horizontal coil former. The components of the RC snubber and the RCD clamp are placed after testing the waveforms of the MOSFET to achieve the best performance of this auxiliary circuits. A mistake taken into account in the second prototype is the thinness and the length of the tracks which is a drawback in terms of EMI.

The second prototype, PCB 2, (figure 6-3) has different objectives, mainly the reduction of the size. But the fulfilment of the isolation regulations and the use of planes and wider tracks are compulsory changes to improve the performance of the whole system.

As it can be appreciated in the figure 6-3 there are two large planes. The upper one is the positive side of the DC bus after the rectification and filtering. The lower one is the ground of the primary which is connected to the source pins of the TNY264GN. The flyback transformer is made by a vertical coil former. The dimensions of the PCB 2 are the same as the 9 V battery, 52.8 mm x 25.8 mm. The external frame, where the holes are made, is removed because it is only a provisional part that acts

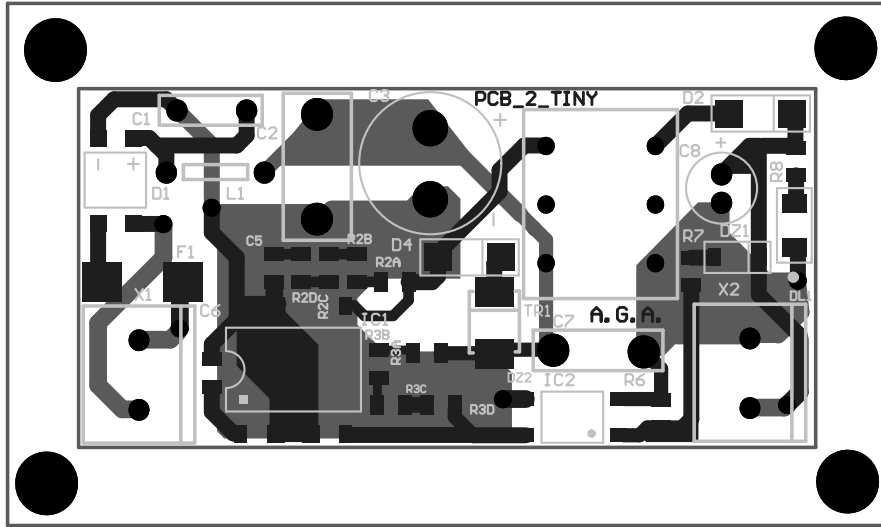


Figure 6-3: PCB 2

as a support.

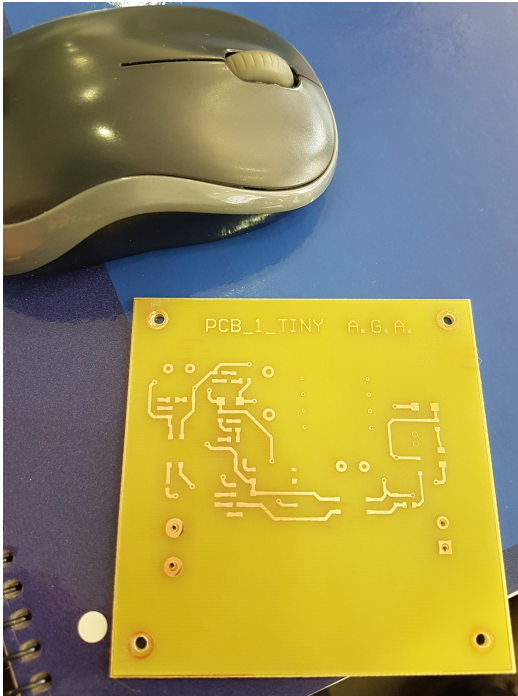
A requirement for the serial manufacture in the production line of the company is also explained. The Surface Mount Device (SMD) components are placed by a pick and place machine, so the components should be welded on the top layer to reduce the manufacture costs. It is also compulsory to keep a distance (4 mm) between through hole components and SMD components welded on the bottom layer because the through hole components are welded by a tin chimney and the closer SMD components can be damaged.

### 6.3 Final prototype

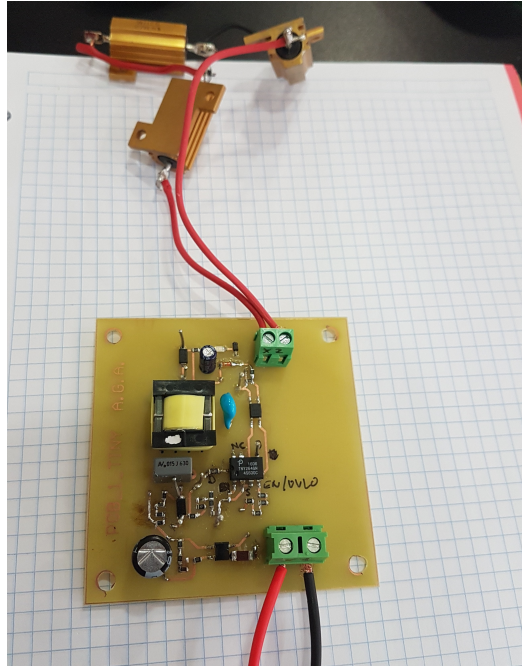
In this section, the pictures of the PCB 1 and PCB 2 are shown in order to appreciate the visual differences of both prototypes.

The figure 6-4a is the board before placing the components on it and the final result of the PCB 1 along with the nominal load is represented in figure 6-4b

The figure 6-5 shows the comparison between the battery and the PCB 2 without any component. As it can be seen the size requirements is perfectly fulfilled.

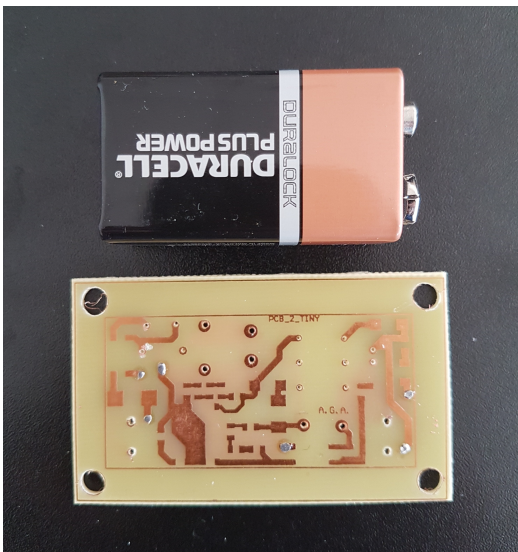


(a) PCB 1 without components.

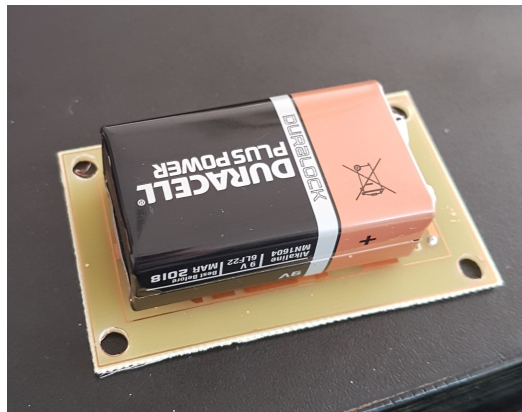


(b) Final result of the PCB 1.

Figure 6-4: Pictures of PCB 1



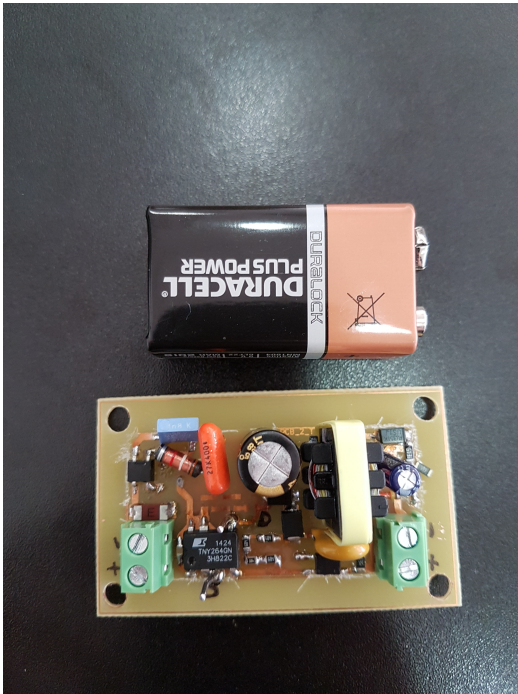
(a) PCB 2 without components



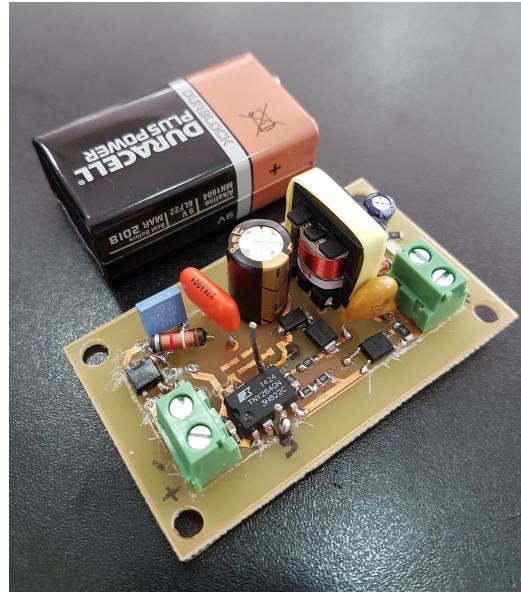
(b) PCB 2 and battery size comparison

Figure 6-5: Pictures of the board for PCB 2

The figure 6-6 represents the final aspect of the PCB 2, the final prototype that works properly and following all the technical requirements.



(a) Final result of the PCB 2.



(b) Final result of the PCB 2.

Figure 6-6: Pictures of final PCB 2

# Chapter 7

## Tests, validation and regulation

In this chapter the tests carried out and the most relevant charts from the oscilloscope are shown explaining the waveform plotted in each one. Then, the tests made by using the LISN are described pointing out the changes made in the circuit from the conclusions reached with these measurements. A thermal and brief study made with the thermal camera is also carried out explaining the possible effects of the temperature and the critical parts of the design. Finally, the measurements taken from the watt-meter are shown and also the validation of the prototype according to the IEC61000-3-2 and IEC61000-4-7 regulations are made in order to see if the design pass the specifications.

### 7.1 Oscilloscope tests

The firsts tests at the oscilloscope are made to visualize and measure the MOSFET turn-off in order to see the resonance waveforms and calculate the complementary circuits like the RC snubber and the clamping circuit. The figure 7-1 shows the the waveforms without complementary circuits, by using only the clamping circuit and by using both of them. The input voltage is 85 V the minimum for this design and the data is collected as .csv and then plotted in MATLAB to compare the performance. As it can be seen, at the 85 V input voltage, the oscillations and the first peak voltage almost reach 600 V, so, at higher input voltage, the TinySwitch would be damaged.

So the clamping circuit is implemented and the peak is removed as the red line shows. However, the resonance still takes place in the system, although it was attenuated by the clamping circuit. To achieve a nearly removal of the resonance oscillations the RC snubber is implemented. The green line shows how the turn-off has now a better performance. This improvement in the waveform is directly related to the harmonics conducted to the grid so it is an important part of the design but it has a cost, the losses in the circuit increase significantly. The reduction in the efficiency is due to these complementary circuits mainly.

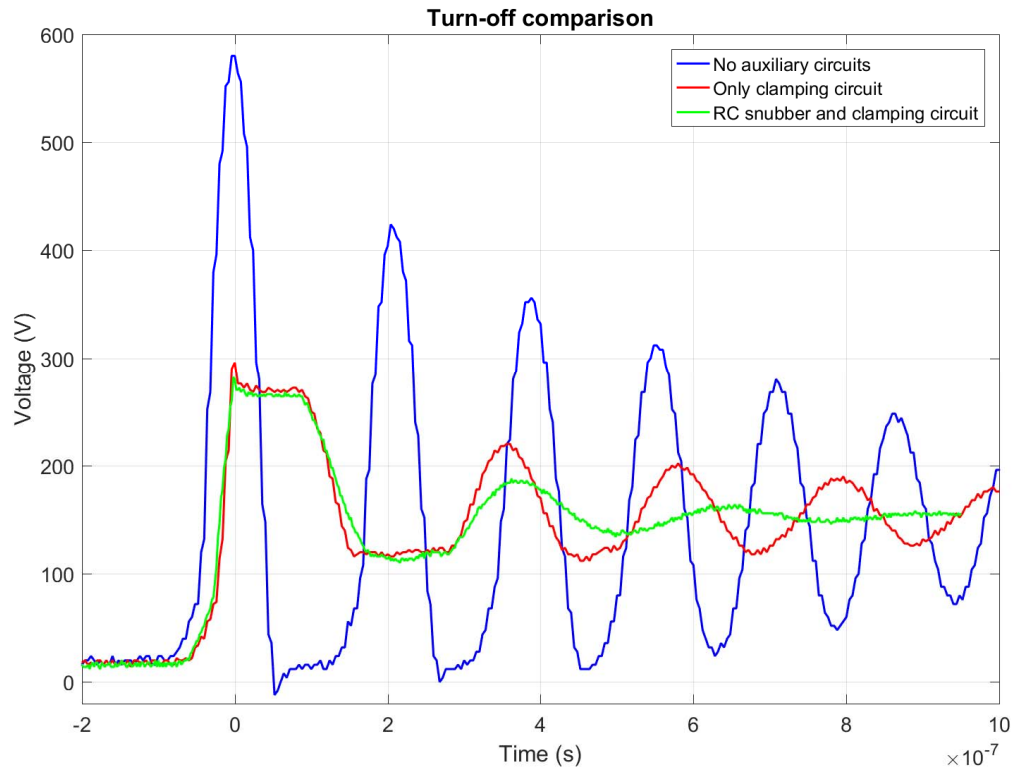
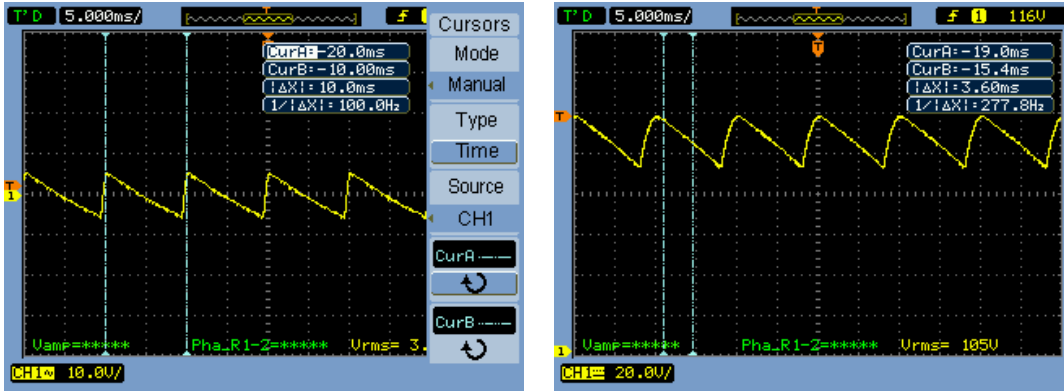


Figure 7-1: Complementary circuits effects at the turn-off

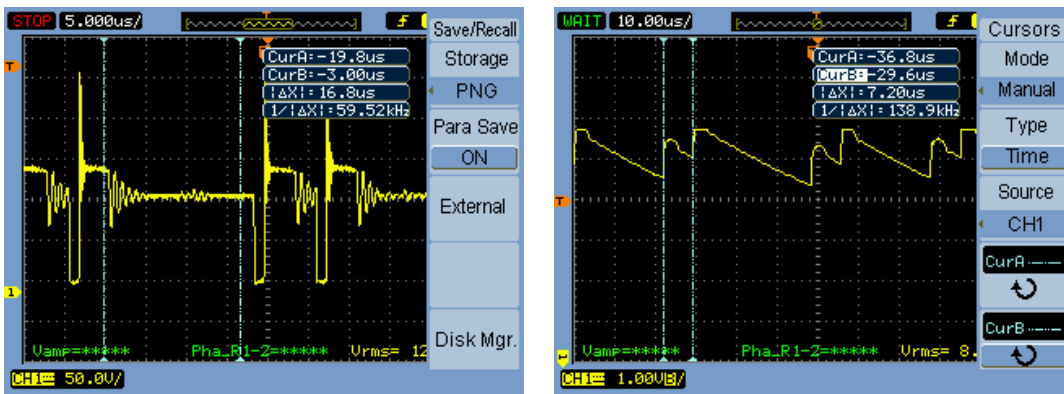
The voltage ripple at the input and the output are also measured in the oscilloscope. The figure 7-2 shows the input voltage ripple at input of 265 V and 85 V, as it is expected has a value between 10 V and 20 V. It can be appreciated that the frequency double than the line frequency, 100 Hz, due to the full-wave rectification of the diode bridge.



(a) Input voltage ripple at 85 V input. (b) Input voltage ripple at 265 V input.

Figure 7-2: Input voltage ripples

The output voltage ripple is also measured at 265 V input. The figure 7-3b shows it pointing out that the higher frequency component comes from the commutation of the MOSFET at 132 kHz. In this case, the cursors indicate 138 kHz, which is within the range of commutation frequency. It can be seen that sometimes the discharge time of the capacitor is larger. It is due the ON/OFF control of the integrated circuit, so the commutation does not take place at all the cycles. This effect can be seen also in the figure 7-3a where some commutations are avoided (figure 7-3).

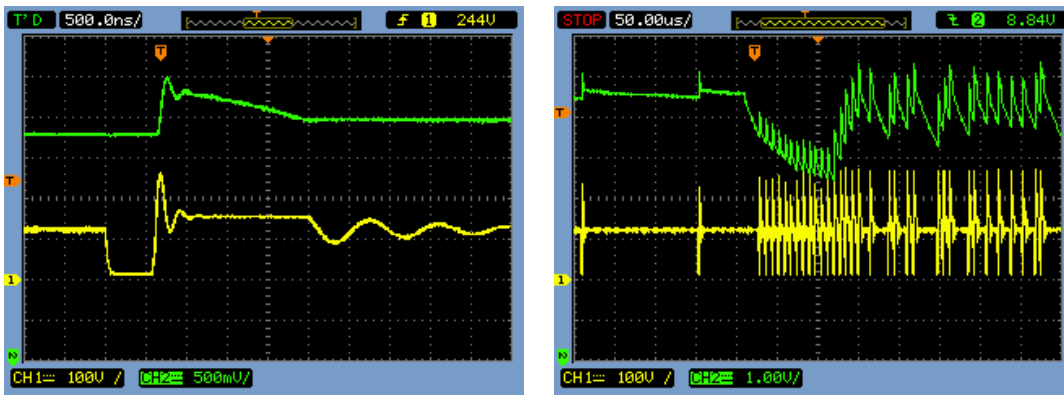


(a) Cycles at 85 V input (b) Output voltage ripple at 265 V input.

Figure 7-3: Detail of ON/OFF control

### 7.1.1 No-load state and transient to ALARM state

The transient from no-load state (NO ALARM at the detector) to load state (ALARM at the detector) is simulated by connecting the nominal load ( $81\ \Omega$ ) of the system which is related to  $9\ \text{V}/1\ \text{W}$ . The figure 7-4 shows that drain-to-source voltage and output voltage transients. First of all, the output voltage gauge (green at the oscilloscope) has a gain of  $1/10$ , so, the division voltage is  $5\ \text{V}$ . It should be pointed out that the output voltage at no-load reaches almost  $10\ \text{V}$  at the turn-off. The transient is clear at figure 7-4b. At no-load the TinySwitch turns-on the MOSFET every  $150\ \mu\text{s}$  ( $6\ \text{kHz}$ ) because it is its typical performance facing a very light load, it avoids some pulses. At a certain moment the system goes to the ALARM state, and as it is expected when the load is connected the output voltage goes down.



(a) Turn-off at no-load and input  $85\ \text{V}$       (b) Transient from no-load to load state

Figure 7-4: Transient to ALARM state

Thus, it is easy to see the reaction of the TinySwitch, it starts working at its maximum frequency to compensate the voltage and then, once it is stable, as the figure 7-5 shows, some cycles are avoided because they are not necessary. During this, zero current state, it can be seen how the capacitor is discharging because it is too small. A bigger capacitor would bring better results in terms of output voltage ripple.

Looking at the table 7.1 a comparison between different measurements carried out with the oscilloscope and the watt-meter. It should be point out the low power consumption at no-load. In a real case, the great part of the time the power is demanded



Figure 7-5: Steady state (ALARM state)

by the sensor at NO-ALARM state (microprocessor, signal adapting circuit, etc.) which is a bit more than the consumption at no load. In case of ALARM the sensor is supposed to absorb 1 W which is the rated power of the power supply designed. It can be appreciated also the relation between peak clamp voltage at the turn-off and the power consumption. In the prototype 1 (PCB 1), the clamping is made at a lower voltage than in the prototype 2 (PCB 2), so, allowing the voltage to rise, the power dissipation decreases. Therefore, a better efficiency and lower temperature is reached in the circuit as it is shown afterwards.

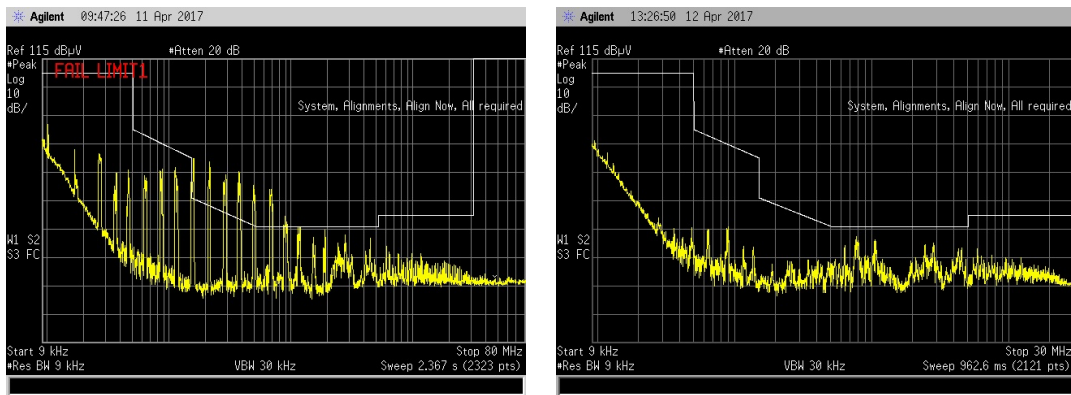
Table 7.1: Comparison PCB1, PCB2 and PCB2 at no-load

	$V_{IN}$ ripple	$V_{OUT}$ ripple	Power	Clamp voltage	$V_{OUT}$	PF
85 $V_{AC}$ load PCB1	4.7 V	0.4 V	1.9 W	213 V	8.89 V	0.54
230 $V_{AC}$ load PCB1	14.32 V	0.46 V	2.1 W	394 V	9.01 V	0.398
265 $V_{AC}$ load PCB1	15.13 V	0.5 V	2.2 W	443 V	9.12 V	0.377
85 $V_{AC}$ load PCB2	5.1 V	0.364 V	1.7 W	296 V	8.92 V	0.51
230 $V_{AC}$ load PCB2	14.51 V	0.413 V	1.9 W	488 V	9.03 V	0.3831
265 $V_{AC}$ load PCB2	15.6 V	0.456 V	2 W	540 V	9.21 V	0.36
85 $V_{AC}$ NO load PCB2	5.1 V	0.058 V	0.098 W	260 V	9.317 V	0.342
230 $V_{AC}$ NO load PCB2	14.52 V	0.226 V	0.249 W	476 V	9.6 V	0.294
265 $V_{AC}$ NO load PCB2	15.58 V	0.239 V	0.290 W	524 V	9.627 V	0.289

## 7.2 Conducted EMI test

The conducted emissions are tested by using the LISN and the spectrum analyzer as it is explained above in chapter 3. Here, the different tests are shown and how they help in the last stages of the design like the input filter design.

The figure 7-6 represents the frequency spectrum with the peak limit before and after the input PI filter implemented at the prototype 1 (PCB 1). Figure 7-6a shows the frequency spectrum of the conducted EMI of the system. In this case, only the Y capacitor is implemented between the primary side positive terminal and the secondary side ground and it can be appreciated the highest magnitude take place at frequency components between 10 kHz and 1 MHz so the PI filter has to be designed based in this frequency range. The figure 7-6b shows the result of implementing the PI filter.



(a) Y capacitor between pri(+) and sec(-)

(b) PI filter implementation

Figure 7-6: Frequency spectrum conducted EMI for PCB 1

The spectrum analyser has based in the regulation CISPR 22, which is analogue to the EN 55022 (no valid now). The regulations which substitute the previous one, are UNE-EN 50561-1 and UNE-EN 55032. The limit represented is the peak limit. The same test are carried out with the PCB 2. It can be seen both limits and, although some frequencies components are higher than the averaged limit, the peak limit is enough to validate the prototype's conducted EMI (figure 7-7).

### 7.3 Thermal study

The temperature reached by the design is measured by using an infra-red camera which indicates where are the components that experiment a higher temperature during the performance and the specific value of temperature.

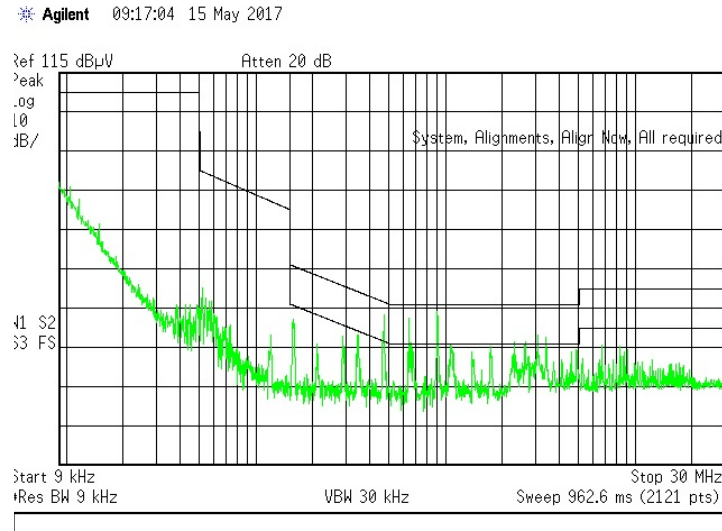
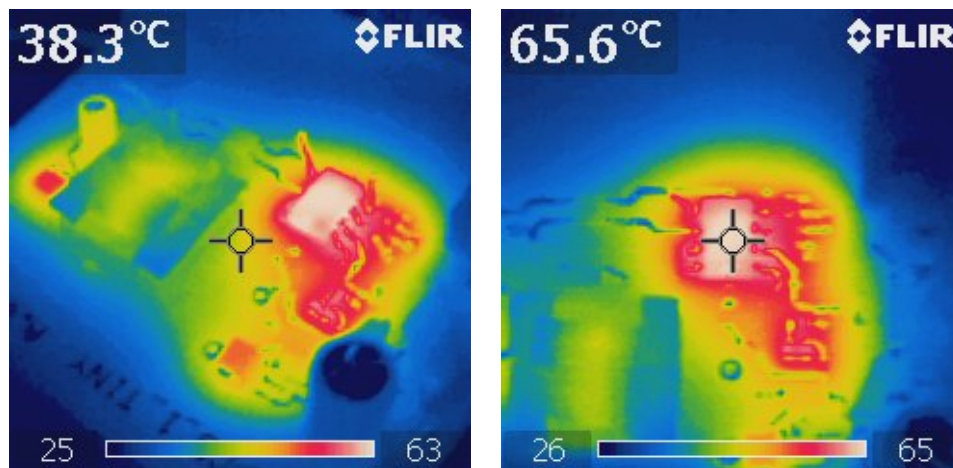


Figure 7-7: Frequency spectrum for PCB 2

The figure 7-8 shows the thermal distribution along the PCB 1. As it can be expected, the maximum temperature is reached at the TinySwitch (figure 7-8b), 65.6°C. The input voltage for this test is 265 V. Other components that suffer high temperatures in the design are the output diode, the diode rectifier and the RC snubber resistors because the highest currents of the design pass through them. Thus, the highest losses also take place at this components.



(a) General vision of the prototype (b) TinySwitch temperature detail

Figure 7-8: Thermal images of the PCB 1

It should be pointed out that neither the flyback transformer nor the capacitors reach high temperatures. The measurements are taken after 30 minutes. The same

test is carried out with the PCB 2 (figure 7-9). The prototype 2 (PCB 2), smaller and with a better layout than the first one, has a similar temperatures pattern. However, focusing in the TinySwitch (figure 7-9b), the temperature reached after 30 minutes is lower, 60.4°C, which implies a improvement in the performance.

In any case, this prototype works with very low power 1 W - 2 W, so the temperature is not a big deal. The margin between the reached temperature and the rated temperature of any of the components is quite wide.

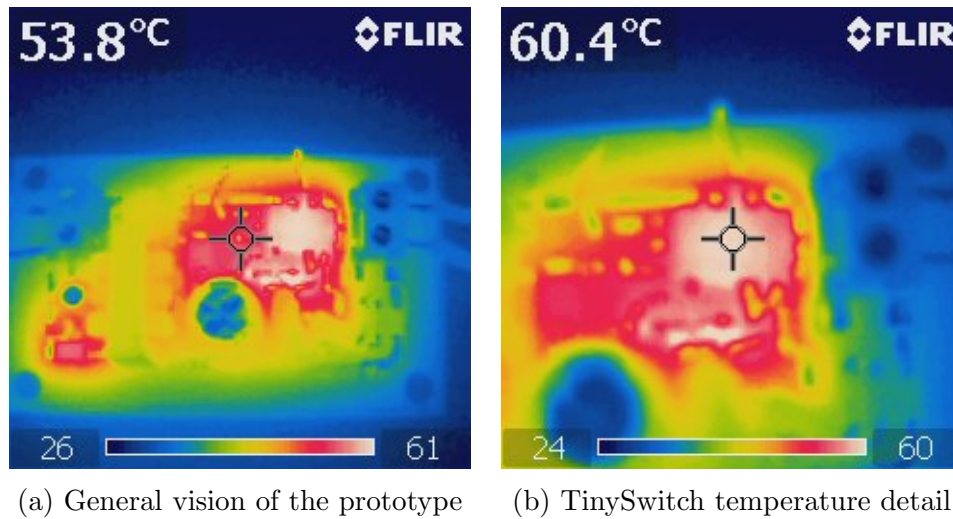


Figure 7-9: Thermal images of the PCB 2

## 7.4 Current harmonics validation. IEC61000-3-2

One of the last tests is made at the watt-meter. This equipment evaluates the harmonics injected in the grid and checks if the prototype fulfil the requirements of the regulation IEC61000-3-2.

Afterwards, all regulations taken into account in the whole project are mentioned and its application in each part of the project is explained.

According to the IEC61000-3-2 or the UNE-EN 61000-3-2 the electrical devices are classified in 4 classes A, B, C and D. The class C is related to the lightning, the class B is related to portable tools. A small power supply can be classified in class D, related to devices with a rated power lower than 600 W like PCs, screens,

refrigerators, etc or in class A, which is valid for any device which can not be classified in the other 3 classes. Thus, the prototype is validated in both classes. The device is connected to grid through the watt-meter which measures voltage and current, and by using a software, an analysis following the regulation is made.

The result is a report (figure 7-10) describing how the tested prototype pass the standard or not.

Looking at the first harmonics of the test in figure 7-10, the measurements are higher than the limits established by the regulation. These limits come from a harmonic current limitation per watt as it is explained in the regulation. Although, in low voltage and power application is difficult to obtain a good performance in terms of harmonics it passes the class D. The class A, which has more robust margins, is also validated for this prototype 2 (PCB 2).

The regulation IEC 61000-3-2 class D has two limits. One related to the current harmonics per watt, where the PCB 2 does not fulfil, and another related to the absolute current harmonics. Thus, the PCB 2 fulfils the second limit and pass the regulation.

The table 7.2 shows the regulations taken into account in this project and passed by the PCB 2 as it are mentioned along the work.

Table 7.2: Regulations validated for PCB 2

Regulation	Title
UNE-EN 14604:2006	Autonomous smoke alarms
UNE-EN 61204-3	Low voltage power supplies with DC output. Part 3: Electromagnetic compatibility
UNE-EN 60065:2015	Audio, video and analogue electronic devices. Security requirements.
UNE-EN 61558-1:2007	Security in power transformers, power transformer, inductors and analogous. Part 1: General requirements and tests (IEC 61558-1:2005).
UNE-EN 60950-1:2003	Information technology devices. Security. Part 1: General requirements
IEC 60384-1:2003	Fixed capacitors for electronic devices uses.
IEC 60384-14:2005	Fixed capacitors for electronic devices uses. Part 14: Intermediate specification: Fixed capacitors fro EMI suppression and grid connection.
UNE-EN 61000-3-2	Electromagnetic compatibility (EMC). Part 3-2: Limits. Harmonic current emissions limits (input current $i = 16$ A per phase devices).
CISPR 22	Information technology equipment. Radio disturbance characteristics. Limits and methods of measurement.

## PCB II (Average)

Print Date : Thu Jun 22 13:30:08 2017  
 MeasureDate : Thu Jun 22 13:26:33 2017  
 Comment : ARMONICOS 230V 50Hz Clase D

Regulation : IEC61000-3-2 Ed3.0 am2  
 IEC61000-4-7 Ed2.0 A1  
 Class : CLASS D  
 MeasureTime : 150.00sec  
 Model : YOKOGAWA WT3000  
 Rating Voltage : 230.00 V  
 Wiring : single-phase 2-wire  
 Element : 1  
 Range : 300V/250mA  
 Current(rms) : 0.0223 A  
 Voltage(rms) : 229.92 V  
 Frequency : 50.000 Hz  
 Power Factor : 0.3824  
 POHC Limit : 0.0008 A  
 POHC Max : 0.0057 A  
 THC : 0.0206 A

PASS

Set Fundamental I : -----  
 Set Power Factor : -----  
 Set P : -----  
 Sigma W Max : 1.9687 W  
 Sigma PF : 0.3824  
 Distortion factor(V) : 0.02 %  
 V THDS : 0.02 %  
 V THDG : 0.02 %  
 Distortion factor(A) : 239.42 %  
 A THDS : 239.42 %  
 A THDG : 239.42 %  
 P THD : 0.02 %  
 Power Limit : 75 W

Order	Measure[A]	Limit[A]	Margin[%]	Order	Measure[A]	Limit[A]	Margin[%]
1	0.0086			2	0.0001		
3	0.0084	0.0067	- 25.9	4	0.0001		
5	0.0081	0.0037	- 117.8	6	0.0001		
7	0.0077	0.0020	- 293.2	8	0.0001		
9	0.0072	0.0010	- 633.9	10	0.0001		
11	0.0066	0.0007	- 860.8	12	0.0001		
13	0.0060	0.0006	- 920.9	14	0.0001		
15	0.0052	0.0005	- 938.3	16	0.0001		
17	0.0045	0.0004	- 916.4	18	0.0001		
19	0.0038	0.0004	- 861.2	20	0.0001		
21	0.0032	0.0004	- 781.4	22	0.0001		
23	0.0026	0.0003	- 687.8	24	0.0001		
25	0.0021	0.0003	- 593.1	26	0.0001		
27	0.0017	0.0003	- 509.7	28	0.0001		
29	0.0014	0.0003	- 448.1	30	0.0001		
31	0.0013	0.0002	- 411.9	32	0.0000		
33	0.0011	0.0002	- 395.9	34	0.0000		
35	0.0011	0.0002	- 388.8	36	0.0000		
37	0.0010	0.0002	- 379.4	38	0.0000		
39	0.0009	0.0002	- 359.9	40	0.0000		

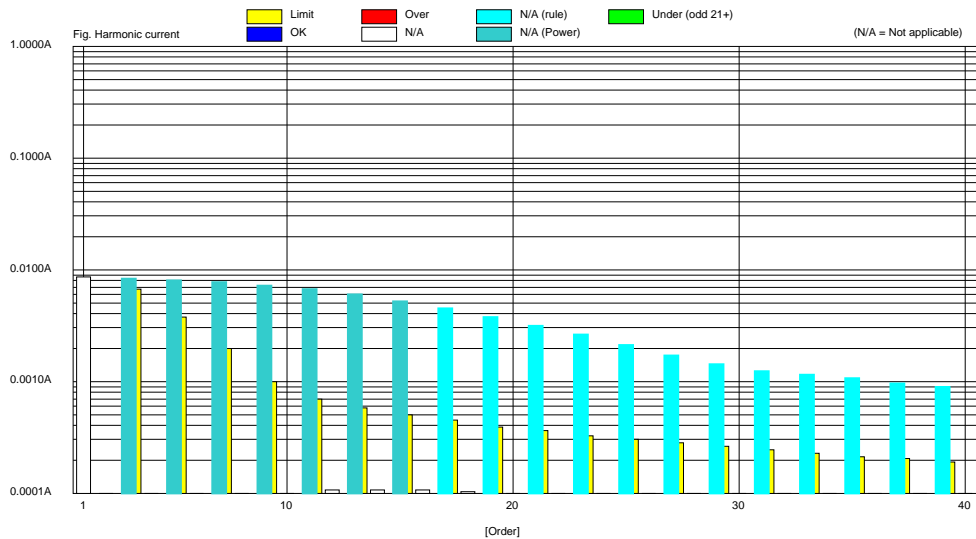


Figure 7-10: Report IEC61000-3-2 class D validation for PCB 2

# Conclusions

Looking at the final results of the project, it can be drawn the following conclusions:

- I have learnt the importance and difficulty of design a power electronics prototype for a company because you have to use the components the company has already bought. This is a severe requirement because limits your decision to some available components at the company warehouse.
- Some difficulties appear during the transformer in terms of obtaining the same values than the theoretical calculation. However, I learnt the whole process of making a home-made flyback transformer which is something that I did not have the opportunity of learning at the university, specially focusing in the isolation regulations like UNE-EN 61558-1:2007.
- It is important the procedure of calculating the complementary circuits (RC snubber and clamping circuit) from testing the design without them. Some authors say that these can be designed by supposing values from the leakage inductance but, for achieving the best performance taking measurements about the resonant frequency at the oscilloscope are needed.
- The results related to the PCB design are satisfactory. The size achieved is the same as the 9 V battery voltage, so the objective is fulfilled. Moreover, the electrolytic capacitors are well chosen in order to increase the lifetime of the prototype.
- The different tests and the regulation is also fulfilled. The regulations related to harmonics injected in the grid are also fulfilled, so the prototype can be

commercialized. The conducted EMI is also within the limits established by the corresponding regulations. It seems easy, but is not a trivial procedure. The low power of the prototype involves an extra difficulty in the achievement of this regulations.

- The company requirements related to the future fabrication are also fulfilled. The needed distance between the SMD components and the through hole components is taken into account to carry out in the future a proper manufacture at the production line.
- To sum up, the whole project is quite satisfactory at all levels although some improvements can be carried out. The future developments section describe the possible enhancements of the prototype.

# Future developments

Although the prototype designed and built during this project is working properly and fulfil the objectives proposed, several enhancements and future works are described in this chapter. Some of them are related to making more studies and tests over the same prototype, replacing components and adding new features to the device.

## A wide study of the integrated circuits

In terms of the components characteristics, it is obvious that there are analogous elements like the FSL206MR from Fairchild that has almost the same internal performance and pin configuration. But also the TEA1721AT from NXP, the NCP1010 from On-Semiconductor, the VIPER06 from STMicroelectronics and the UCC28910. All off them, could be a good solution instead of the TinySwitch, but the schematic could need a revision and surely, a new design. Thus, a future task would be designing different PCBs for each integrated circuit and testing them in order to make a wide study and decided what is the better solution for our application.

## Study of the Flyback Transformer

The magnetic core used in this work and flyback transformer design can be studied deeply. With and without looking at the price, there are several shapes and materials for the magnetic cores that are able to be used in this application. A smaller transformer may be analysed and tested in the future in order to reduce the size of the prototype and to increase the efficiency, although it would mean raising the price

of the prototype.

## **Electrolytic-Less solutions**

It is a trend nowadays in power electronics. The removal of the electrolytic capacitors is a significant challenge for all the electronics engineers because of the short life they have in comparison with the rest of the typical components of a design. A future task would be redesign the prototype trying not to increase so much the size and to remove the electrolytic capacitors from it. However, it is a hard work and it is not straightforward at all.

## **Smoke detector features**

As the regulation says that an autonomous smoke detector which is connected to the grid, also needs an auxiliary power supply from a battery when a grid fault takes place. Thus, a battery charger can be designed and a complete control system for switching between both power supply options. With this additional system the whole smoke detector would fulfil all the specification of the regulations and it could be commercialized.

# Quality report

The stay in NormaGrup Technology S.A. was very gratifying from the first day I started the intern-ship because the people was very polite and thoughtful with me. The company co-advisor show me all the production process from the beginning at the R and D department, to the serial production, the mechanical department and the plastic injection department. Moreover, any of the R and D department workmates made themselves available for any problem or doubt I could have.

In terms of coordination between the company co-advisor and the advisor was fluent because the co-advisor was a student years ago and the advisor was his professor in some subjects. Even so, I was the nexus between them, asking the co-advisor technical issues and requirements of the project and asking the advisor issues related to the document, focusing on the concepts and the format of the thesis.

The work carried out was directly related to master thesis generally. Some days I was required for helping a workmate that was taking measurements of a device or was making some tests. I also helped them with the installation of the new industrial unit of the company, where the new R and D department was established. I spent the last month at the new building which is more modern and spacious.

Regarding the management of the Master Thesis was very simple and straightforward. The person which is in charge of receiving the payment letter was very polite with me. The coordinator of the master was also very thoughtful with me, any question I had was answered by him as soon as he read the email. Moreover, he sent us all the procedure for the structure and the presentation of the master thesis which make me easy the



# Internship at NormaGrup Technology S.A.

Most of the time during intern-ship, I was developing my Master's Thesis but also I have been helping at other activities inside the company. The electronics technician measured the smoke detectors and I had to assist them while they calibrated the sensor. I was also carrying out water IP tests at the hermetic water chamber in order to check if a light case model, called Hermetic, allows the water go inside it.

Every week tests related to the duration of the batteries installed in the different emergency lights was made. I also participated in the measurements wrote down the times when the lights turned-off. This measurements was coordinated by the Quality Department.

I also helped a technician with a welding process of some LEDs. I got some PCBs with the LEDs put in their pads, each one of them with welding paste spread over the pad area. I went to the production line at 2 p.m., when the production is stopped, and I introduced one by one the PCBs into the oven in order to fix all the LEDs to the boards.

One day, a workmate, called Fernando, showed me the whole fabrication process and the facilities of the company. From the warehouse where all the components, materials and also the final products are stored. Then, the mechanical department where the moulds are made properly for be used, then, in the injection plastic department. In this section, all the cases of the lights and products are manufactured.

When the cases are fabricated, it is the time of the production line. There is two production lines in the main building of the business group. At the beginning of the

production chain the specific warehouse of the electronics components are installed. The process is the following:

- The PCBs are empty
- The tin is spread over all the board and it only remains on the copper zones.
- The pick and place machine place all the components.
- Then, a temperature cycle weld the components from 160° to 240°. After this, the PCB has to be straightened.
- The through hole components are placed and welded.
- The operators take the PCBs and place it into the ABS plastic cases to complete the process.

The most popular product is an emergency light called Dunna which is widely used in our country. Every day is manufactured in the company.

Finally, the stay in NormaGrup Technology S.A was very satisfactory both at academic level and a professional and personal level.

# Bibliography

- [1] Aluminum electrolytic capacitor application guide. Technical report, Cornell Dubilier Capacitors.
- [2] Differential and common mode noise. Technical report, Murata.
- [3] Power supply technical guide 2010/2011. Technical report, XP Power.
- [4] TinySwitch flyback design methodology. Technical report, Power Integrations, Inc., World Headquarters Americas, Hellyer Avenue, San Jose, USA, 1999.
- [5] Topswitch power supply design techniques for EMI and safety. Technical report, Power Integrations, 2005.
- [6] Transil clamping protection mode. Technical report, ST Microelectronics, 2014.
- [7] Sam Abdel-Rahman. Resonantllc converter:operation and design. Technical report, Infineon Technologies North America (IFNA) Corp., 2012.
- [8] Schneider Electric. Detectores humo, gas e inundacion, 2017. <https://www.schneider-electric.es/es/product-range/>.
- [9] Robert W. Erickson. Supplmentary notes on emi and layout fundamentals for switched-mode circuits. Technical report, University of Colorado.
- [10] GOLMAR. Golmar products, 2017. <http://www.golmar.es>.
- [11] Alfred Hesener. Electromagnetic interferences in power supplies. Technical report, Fairchild Semiconductor, 2011.
- [12] Power Integrations. *TNY263-268 TinySwitch-II Family*. Power Integrations, World Headquarters Americas, Hellyer Avenue, San Jose, USA, August 2016.
- [13] Sanjaya Maniktala. Aluminum cap multipliers - why we can't have them and eat them too. Technical report, National Semiconductor Corp., 2004.
- [14] MIRA. Autonomous smoke detectors, 2017. <https://securimport.com/detector-de-humo-autonomo-de-con-pilas-con-salida-de-alarma-p-2886/>.
- [15] Jean Picard. Under the hood of flyback SMPS designs. Technical report, Texas Instruments, 2011.

- [16] Ray Ridley. Flyback converter snubber design. *Designers Series XII, Switching Power Magazine*, 2005.
- [17] Ray Ridley. Ridley engineering, 2017. <http://www.ridleyengineering.com/design-center-ridley-engineering>.
- [18] RS. Rs components, 2017. <http://uk.rs-online.com/web/p/embedded-switch-mode-power-supplies-smps/7719382/>.
- [19] COFEM S.A. Cofem products, 2017. <http://www.cofem.com/productos/>.
- [20] NormaGrup Technology S.A. Normadet, 2017. <http://www.normadet.com/>.
- [21] VisioTech. Smk- 500. smoke detectors, 2017. <https://www.visiotechsecurity.com/es/productos/intrusion/chuango/detectores>.
- [22] Flyback converter, lecture notes ECEN4517. University of Colorado.